

Author response to reviewers (RC1, RC2), written by Marc D. Mallet on behalf of all authors. Reviewer comments are indicated in bold, author comments are indicated in normal text and sections taken from the manuscript are indicated in italics.

RC1.

The manuscript of Mallet et al. presents chemical composition and size distribution measurements conducted at the island of Lampedusa, Italy during a one-month period in the summer of 2013. It occurs that ammonium sulfate is the main contributor (63%) to the submicron non-refractory mass, followed by organics (33%). By performing Positive Matrix Factorization (PMF) analysis on the derived organic aerosol mass spectra it occurs that there are four factors contributing to the total organic aerosol, namely a hydrocarbon-like OA, a methanesulfonic acid-related OA, and two oxidized OA, a more oxidized and a less-oxidized one. The two secondary OOA factors contribute the most (more than 80%) to the total OA, but with having different origin. The more-oxidized was observed during easterly air masses from the eastern Mediterranean and central Europe while the less-oxidized during westerly winds from the western Mediterranean, the Atlantic Ocean and high altitudes over France and Spain from mistral winds. Finally, an attempt is made to investigate the aging of aerosols by comparing concurrent measurements at Lampedusa and Corsica, revealing a dependence on travel time between the two sites and an enhancement of organics (40%) and a significant increase in sulfate and ammonium (by a factor of 6 and 4, respectively) between Ersa (Corsica) and Lampedusa.

The paper is well written and easy to follow, though there are some issues and more thorough discussion should be made in specific sections. A very interesting point of the study is the study of the aging aerosol gradient and its dependence on the time travel of the air masses between Corsica and Lampedusa. Other than that the paper can be recommended for publication after addressing the issues listed below.

Authors: The authors would like to thank the reviewer for her/his time and helpful comments. The reviewer's main concerns were surrounding the lack of reported details surrounding the c-ToF-AMS measurements and data analysis and comparisons made between the cToF-AMS, SMPS and PILS measurements. We address these specific comments in the following section, "Specific comments:".

In addition to the changes outlined below, several other changes in the manuscript have been made (e.g. reference formatting, typos). The major change is that data presented in Table 1 and Supplementary Table S1 has now been combined and displayed in a new figure (Figure 8; see below). This figure summarises the PM₁ composition from all of the previous studies around the Mediterranean basin that have performed a PMF analysis. This new Figure makes it much easier to compare the results of our study to these previous studies by visualising the composition with pie charts pointing to the sampling location, rather than presenting the data in tables. Subsequent Figure and table numbers have been updated.

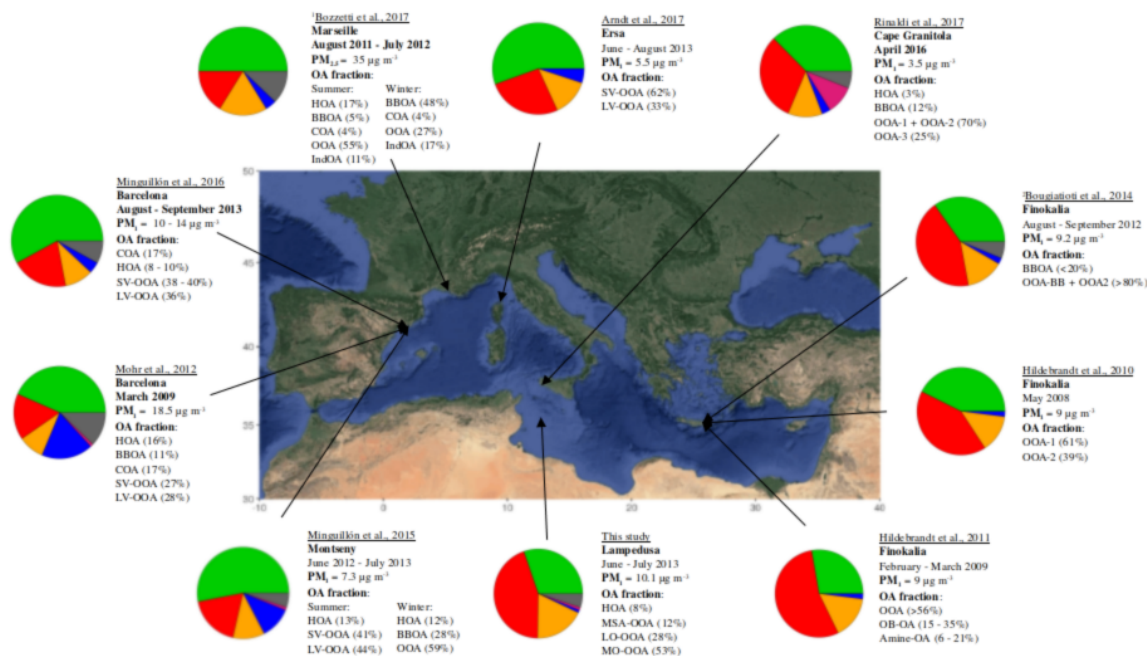


Figure 8 A summary of studies that have investigated NR-PM₁ composition (including PMF of OA) around the Mediterranean basin. Only studies that have investigated PMF-based OA source apportionment are reported. Pie charts display the average concentration during each study where green corresponds to organics, red to sulphates, orange to ammonium, blue to nitrate, pink to either chlorides or sea salt and black to elemental or black carbon. The OA fraction acronyms correspond to the following: HOA: Hydrocarbon-like Organic Aerosol, SV-OOA: Semi-volatile oxygenated Organic Aerosol, LV-OOA: Low-volatility oxygenated Organic Aerosol, BBOA: Biomass burning Organic Aerosol, COA: Cooking Organic Aerosol, OOA: Oxygenated Organic Aerosol, F4: "Factor -4" (unidentified PMF factor), IndOA: Industry-related Organic Aerosol, OB-OA: "Olive-branch Organic Aerosol. See Supplementary Tables S1 and S2 for further details about the sampling locations, instruments used and pie chart values. ¹This study collected on PM_{2.5} filters and nebulised into an HR-ToF-AMS. ²Excludes fire-periods.

Specific comments:

1) More information about the c-ToF-AMS measurements and data analysis should be provided: - Response Factors and/or Relative Ionization Efficiencies of the different species. Was there a collection efficiency correction applied?? Was a constant CE used or a chemical composition dependent one e.g. Middlebrook et al. (2012)?

Also I would suggest creating a separate section after Section 2.2 as Quality control/Quality assurance of the measurements where I would include the comparisons between PM₁ from chemical composition and SMPS, sulfate from c-ToF-AMS and PILS and the supporting measurements from the nanoMOUDI.

Authors: More detail has been given for the c-ToF-AMS measurements and data analysis in both sections 2.2 Instrumentation, measurements and data, and 2.3.1 Analysis of the cToF-AMS data. We did not include a separate QA/QC section but instead provided more detailed comments in the Experimental and Results section regarding the cToF-AMS measurements and comparisons between the SMPS and PILS.

With regards to the c-ToF-AMS ionization calibrations, relative ionization efficiencies and collection efficiencies, the following paragraph as been included in Section 2.2:

“The ionization efficiency (IE) with respect to nitrate anions was calculated every 5-6 days using nebulised 350 nm mobility diameter ammonium nitrate particles (values varied between 1.42×10^{-7} and 1.53×10^{-7}). The relative IE (RIE) of ammonium was slightly higher than the default value and was 4.3 based on the mass spectrum of ammonium nitrate data from IE calibrations. The RIE of sulfate was determined by comparing the theoretical and the measured concentration of a solution of ammonium nitrate and ammonium sulfate and was determined to be the default value of 1.2. For the organic fraction, the default value of 1.4 was used. For each of the major species, a composition dependent collection efficiency was applied as proposed by Middlebrook et al., 2012 and was on average 0.549, very similar to the default value of 0.55.”

Further detail of the sea salt estimation has also been provided:

“The PM1 sea salt concentration was estimated in the cToF-AMS by applying a scaling factor of 102 to the ion fragment (using the cumulative peak fitting analysis described in Muller et al., 2011) at 57.98 assigned to NaCl as proposed by Ovadnevaite et al., 2012. This scaling factor was determined by nebulising monodisperse 300 nm (mobility diameter) NaCl particles into the cToF-AMS and comparing the NaCl⁺ signal to the total mass calculated using the number concentration from a CPC-3010. This calibration was done after the campaign but with similar tuning conditions. The sea salt-SO₄²⁻ (ss-SO₄²⁻) was calculated as $0.252 \times 0.3 \times [\text{seasalt}]$, where 0.252 is the mass ratio of SO₄²⁻ to Na⁺ in sea salt and 0.3 is the mass ratio of Na⁺ to sea salt (Ghahremaninezhad et al., 2016). Given these assumptions, the uncertainty in the seasalt concentrations are likely to be significantly higher than the typical 20%, although the total contribution of seasalt to the PM1 fraction was very small ($0.30 \mu\text{g m}^{-3}$; <4 %).”

2) On multiple occasions in the manuscript the term “agreement” is mentioned, but no actual metric is provided. For example, in L307 “reasonable agreement between the PM1 concentration calculated from composition measurements and the SMPS” is stated, but what does this translate to? Apart from the timeseries, no scatter plot is provided, no correlation coefficient, therefore how is this agreement defined? Same in L312.

Authors: The reviewer is correct that “agreement” is too loose of a term. The first instance when it is used:

“reasonable agreement between the PM1 concentration calculated from composition measurements and the SMPS...”

Now reads as:

“There was reasonable agreement (slope = 0.62; $R^2 = 0.67$) between the PM1 mass concentration calculated from composition measurements and the SMPS...”

The second instance of when it was used:

“For most of the campaign there was a good agreement between the $PM_1 SO_4^{2-}$ and the TSP SO_4^{2-} concentration, with the exception of periods of high sea salt concentrations when the TSP SO_4^{2-} were significantly higher (see Supplementary Figure S2).”

Now reads:

“During most of the campaign there was a reasonable agreement (slope = 1; $R^2 = 0.6$) between the $PM_1 SO_4^{2-}$ (c-ToF-AMS) and the TSP SO_4^{2-} (PILS) concentration, with the exception of periods of high sea salt concentrations when the TSP SO_4^{2-} were significantly higher (slope = 0.5; $R^2 = 0.2$ for TSP Cl^- concentrations $> 10 \mu g m^{-3}$; see Supplementary Figure S2).”

Technical corrections:

L76 I would also add here the references of Bougiatioti et al. (2014) and Minguillon et al. (2015) as identifying biomass burning aerosol in the Mediterranean during summer

Authors: These references have been added. The sentence now reads :

“Furthermore, biomass burning aerosol has frequently been observed over the basin, in particular the dry season in summer when forest fires are more common (Bougiatioti et al., 2014; Minguillon et al., 2015; Pace et al., 2005).”

L126 change to “BBOA”

Authors: The incorrectly labelled “BBA” has been changed to “BBOA”.

L140 secondary sites established (delete “were”)

Authors: The incorrect use of “were” has been deleted. The sentence now reads:

“Numerous secondary sites established along the Mediterranean coasts in Spain, Italy and Corsica beyond the SOP-1a have also provided valuable knowledge of the atmospheric composition in the western and central Mediterranean regions (Chrit et al., 2017; Chrit et al., 2018; Becagli et al., 2017).”

L162 probably you mean Total Suspended Particulate (TSP)

Authors: “Total Suspected Particulate (TPS)” has been changed to “Total Suspended Particulate (TSP)”.

L165 check font style

Authors: All fonts throughout the manuscript have now been made consistent.

L157-164 More information on the c-ToF-AMS measurements should be provided here

Authors: As detailed above, more details about the c-ToF-AMS measurements have been provided (IE, RIE, CE, seasalt scaling).

L299 Dry NR-PM1? There is nothing mentioned about using a dryer in the instrumentation section (2.2)

Authors: A nafion drier was used. The relative humidity at the AMS inlet was logged for ~ half of the campaign and was below 55%. This has been indicated in Section 2.2:

“A nafion drier was used, however the relative humidity at the inlet of the c-ToF-AMS was checked throughout the campaign and was always below 55%.”

L307 Reasonable agreement meaning what? R2 of how much?

Authors: As described above, a slope and correlation coefficient for the PM1 from the cToF-AMS and SMPS has now been provided:

“There was reasonable agreement (slope = 0.62; $R^2 = 0.67$) between the PM1 mass concentration calculated from composition measurements and the SMPS...”

L312-314 Do you mean between c-ToF-AMS and PILS? If yes I would suggest to change and state the methods used, preferably also give a correlation coefficient

Authors: As described above, a slope and correlation coefficient has been provided. We have also indicated the instrument used (c-ToF-AMS and PILS):

“During most of the campaign there was a reasonable agreement (slope = 1; $R^2 = 0.6$) between the PM1 SO_4^{2-} (c-ToF-AMS) and the TSP SO_4^{2-} (PILS) concentration, with the exception of periods of high sea salt concentrations when the TSP SO_4^{2-} were significantly higher (slope = 0.5; $R^2 = 0.2$ for TSP Cl- concentrations $> 10 \mu g m^{-3}$; see Supplementary Figure S2).”

L340 low-volatility/ highly oxidized L340 Make title bold

Authors: This has been fixed. “typical of low-volatile/highly oxidized OOA” now reads as “typical of low-volatility/highly oxidized OOA”.

L511-516 Night-time nucleation events have also been observed in the Eastern Mediterranean (Kalivitis et al. 2012)

Reference

Kalivitis, N., Stavroulas, I., Bougiatioti, A., Kouvarakis, G., Gagné, S., Manninen, H. E., Kulmala, M., and Mihalopoulos, N.: Night-time enhanced atmospheric ion concentrations in the marine boundary layer, *Atmos. Chem. Phys.*, 12, 3627-3638, <https://doi.org/10.5194/acp-12-3627-2012>, 2012

Authors: This has now been included and referenced:

“Night-time NPF events have also been observed in the Eastern Mediterranean (Kalivitis et al., 2002).”

RC2

This study presents results on composition of fine PM fraction (approx. PM₁) in Lampedusa, an island site in the southern central Mediterranean), by using a cToF-AMS. Results were obtained during the first CHARMEX Special Observation Period (SOP1) in summer 2013. Results were compared with similar studies performed in the Mediterranean region in different periods and specifically with those obtained at Ersa site, Corsica, during the sampling period. The novelty of this work lies in the fact that it is the first study of this type carried out on an island in the central Mediterranean. One of the main concerns of this study is the short duration of the sampling period (less than one month). This can affect its representativeness, the comparison with other studies and the interpretation of the results. However, results can be considered of interest in the framework of the CHARMEX SOP1.

Variations in PM₁ composition are interpreted as a function of the origin of air masses. Higher concentrations of sulfate were obtained during transport from eastern Mediterranean, probably due to the impact of emissions from this region. A clear variation was also observed for the LO-OOA/MO-OOA ratios, with a higher contribution of the most oxidized aerosols with transport from the east.

Authors attempt to study the aging of aerosols during transport by comparing PM₁ composition at Lampedusa and Ersa, when affected by the “same” air masses. Comparison was performed for the different clusters defined. This comparison was mainly focused on sulfate; differences were related to the accumulation of SO₄ and the SO₂ conversion (mainly related to the shipping emissions). A significant increase was obtained for sulfate concentrations during transport of air masses from the East. As shown in Figure 13, during transport from eastern Mediterranean, it seems that the Lampedusa site is affected by other air masses different to those impacting at Ersa. Thus, higher concentrations of sulfate at Lampedusa may be related to the impact of air masses from the East, that are not impacting at Ersa. Therefore, the proposed methodology has some limitations for estimating the aging under these scenarios.

The authors thank the reviewer for her/his time in reviewing the manuscript and their suggestions. Many of the reviewers comments were regarding small technical/grammatical errors which have been addressed (and described in more detail below). The reviewer has two larger concerns regarding the representativeness of the study period as well as the conflation of aging processes with the possible influence of different air masses

The reviewer’s first concern is regarding the short duration (less than one month) of the field campaign, although she/he acknowledges the scope of the study within the broader framework of Charmex. Due to the scale and logistics of studies such as this one with extensive instrumentation, it is extremely difficult and expensive to perform longer-term measurements. Comparable studies which are summarised in this study (see updated Figure

8) are also of a similar length, with the exception of those on continental Europe that are more easily accessible. Furthermore, while we agree that the length of the campaign period is not enough to measure longer term climatology or seasonality, the link between the aerosol composition and size and the air mass back trajectory cluster analysis provides some detail about how the wider synoptic conditions could influence the aerosol composition at Lampedusa. The authors do agree though that long term (multi-seasonal or multi-year) measurements at remote sites would be very valuable.

The reviewer's second concern is regarding the comparisons between the sulphate concentrations measured concurrently at the Lampedusa and Ersa sites and the limitations of the methodology to estimate aging between the two sites. The reviewer is correct in that we do not know if there is an aging process (e.g. $\text{SO}_2 \rightarrow \text{SO}_4^{2-}$) between the two sites or if there are other air mass from the east that are impacting the sulphate concentrations. In order to address this concern, we have changed the title of the section from: "*3.6 Evidence of aging across the Mediterranean*" to "*3.6 Accumulation of sulphates across the Mediterranean*". We have also changed instances when "growth" of sulphate to "accumulation" of sulphates which is more agnostics about the origin and mixing state of the sulphate aerosol. Lastly, we have changed the following sentence: "*It is expected that the accumulation of sulphate would increase as the total travel time increases due to the opportunity for SO2 conversion.*" to: "*It is expected that the accumulation of sulphate would increase as the total travel time increases due to the opportunity for SO2 conversion or from the addition of sulphate from separate air masses which are not accounted for in the HYSPLIT model.*".

In addition to the Minor changes outlined below, several other changes in the manuscript have been made (e.g. reference formatting, typos). The major change is that data presented in Table 1 and Supplementary Table S1 has now been combined and displayed in a new figure (Figure 8; see below). This figure summarises the PM_{10} composition from all of the previous studies around the Mediterranean basin that have performed a PMF analysis. This new Figure makes it much easier to compare the results of our study to these previous studies by visualising the composition with pie charts pointing to the sampling location, rather than presenting the data in tables. Subsequent Figure and table numbers have been updated.

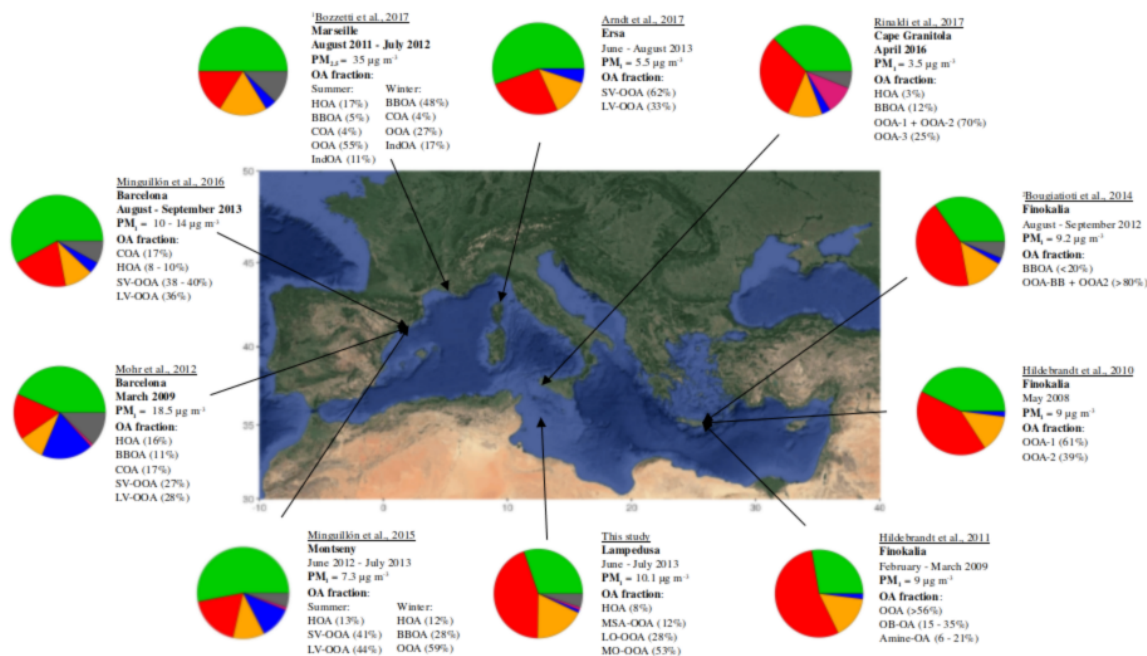


Figure 8 A summary of studies that have investigated NR-PM₁ composition (including PMF of OA) around the Mediterranean basin. Only studies that have investigated PMF-based OA source apportionment are reported. Pie charts display the average concentration during each study where green corresponds to organics, red to sulphates, orange to ammonium, blue to nitrate, pink to either chlorides or sea salt and black to elemental or black carbon. The OA fraction acronyms correspond to the following: HOA: Hydrocarbon-like Organic Aerosol, SV-OOA: Semi-volatile oxygenated Organic Aerosol, LV-OOA: Low-volatility oxygenated Organic Aerosol, BBOA: Biomass burning Organic Aerosol, COA: Cooking Organic Aerosol, OOA: Oxygenated Organic Aerosol, F4: "Factor -4" (unidentified PMF factor), IndOA: Industry-related Organic Aerosol, OB-OA: "Olive-branch Organic Aerosol. See Supplementary Tables S1 and S2 for further details about the sampling locations, instruments used and pie chart values. ¹This study collected on PM_{2.5} filters and nebulised into an HR-ToF-AMS. ²Excludes fire-periods.

Minor changes

Line 99 (e.g. FLEXPART; (Stohl et al., 2005))

Authors: A closing bracket has been added - "(e.g.FLEXPART; (Stohl et al., 2005))" now reads "(e.g. FLEXPART; (Stohl et al., 2005))".

Line 108: (PMF; (Paatero, 1997; Paatero and Tapper, 1994))

Authors: A closing bracket has been added - "(PMF; (Paatero, 1997; Paatero and Tapper, 1994))" now reads "(PMF; (Paatero, 1997; Paatero and Tapper, 1994))".

Lines 144-146: is the first "detailed characterization" in the Central Mediterranean, at Lampedusa, or during the CHARMEX project?

Authors: It is the first detailed characterization of PM₁ in the central remote Mediterranean in general. The sentence has been changed from:

"In this paper, we present the first detailed characterisation of PM₁ in the central Mediterranean region from measurements of size-resolved chemical composition from the island site of Lampedusa during the ChArMex/ADRIMED SOP-1a."

and now reads

“In this paper, we present the first detailed characterisation of PM1 in the central remote Mediterranean region, using measurements of size-resolved chemical composition on the island site of Lampedusa during the ChArMex/ADRIMED SOP-1a.”

Line 162: Please, indicate the sampling flow

Authors: The sample flow of the TSP (16 lpm) has now been indicated.

Line 167: for major inorganic and organic. . .

Authors: This has been fixed. “Samples were analysed for major and organic anions...” now reads as “Samples were analysed for major inorganic and organic anions...”

Line 175: please indicate flow for MOUDI; did you use the same TSP inlet for all the instruments?

Authors: The flow rate for the MOUDI cascade impactor (10 lpm) has been provided. A TSP inlet was used for the MOUDI, PILS, c-ToF-AMS and SMPS which has now been explicitly stated in the respective descriptions of each inlet.

Line 177: which kind of filters did you use?

Authors: PTFE (2 µm pore size) and coated with high quality vacuum grease (Dekati DS-515) to avoid bouncing. This has now been indicated.

Line 179: Denjean et al. (2016)).

Authors: This has been fixed. “Denjean et al., (2016)) now reads as “Denjean et al., (2016).”

Line 214: by (Ovadnevaite et al., (2012)).

Authors: This has been fixed. “...as proposed by (Ovadnevaite et al., 2012)” now reads as “...as proposed by Ovadnevaite et al., 2012.”

Line 215: High uncertainty estimation of the sea salt

Authors: The high uncertainty estimated of the sea salt has been explained in more detail, although it was not quantified during the experiment. The section regarding the sea salt estimation now reads :

“The PM1 sea salt concentration was estimated in the cToF-AMS by applying a scaling factor of 102 to the ion fragment (using the cumulative peak fitting analysis) at 57.98 assigned to NaCl as proposed by Ovadnevaite et al., 2012. This scaling factor was determined by nebulising monodisperse 300 nm (mobility diameter) NaCl particles into the cToF-AMS and comparing the NaCl⁺ signal to the total mass calculated using the number concentration from a CPC-3010. This calibration was done outside of the campaign but with similar tuning

*conditions. The sea salt-SO₄²⁻ (ss-SO₄²⁻) was calculated as 0.252 * 0.3 * [seasalt], where 0.252 is the mass ratio of SO₄²⁻ to Na⁺ in sea salt and 0.3 is the mass ratio of Na⁺ to sea salt (Ghahremaninezhad et al., 2016). Given these assumptions, the uncertainty in the seasalt concentrations are likely to be significantly higher than the typical 20%, although the total contribution of seasalt to the PM₁ fraction was very small (0.30 µg m⁻³; <4 %). Samples were analysed for major and organic anions”*

Line 299: please, specify the time period of the concentrations (hourly basis; 30 minute?)

Authors: the mean was calculated using the instrument time resolution of 3 minutes.

Lines 312, 313, 314, 565: SO₄²⁻

Authors: There were four instances when the sulphate anion was mistakenly written with a “+” instead of “-”. These instances of SO₄²⁺ have been changed to SO₄²⁻.

Line 314: (see Supplementary Figure S2).

Authors: This has been fixed. “(see Supplementary Figure S2.” now reads as (see Supplementary Figure S2).”

Lines 319-322: this is estimation, more measurements, for a wider period are necessary for demonstrating this.

Authors: The reviewer is correct. The wording has been altered to keep it appropriate to the scope of the study.

“This indicates that, in these circumstances, the sea salt particles acted as a condensation sink for sulphate precursors. This has important implications for the radiative properties of these aerosols by altering the scattering properties and, potentially cloud condensation nuclei concentrations and composition.”

Has been changed to:

“If these events are frequent, this could have important implications for the radiative properties of these aerosols by altering the scattering properties and, potentially cloud condensation nuclei concentrations and composition.”

Lines 416-418: This comparison will depend on the sampling periods. This study was performed in summer, where high concentrations of sulfate are expected. The study by El Haddad et al (2013), also in summer, showed higher concentration of sulfate than OA

Authors: The following sentence has been removed:

“Furthermore, the contribution of ammonium sulphate was higher in this study than of all those undertaken in the eastern Mediterranean basin, highlighting the role contribution of sulphates across the Mediterranean.”

This original sentence was based on the reported ammonium sulphate concentrations in this study and those from around the Mediterranean basin and was supposed to point out that those in this study were higher than *western* (not eastern as initially stated) Mediterranean. Although as the reviewer points out, making this comparison depends on the sampling periods which are not always in the same season. A more detailed study of local SO₂ sources near each of the sites would be beneficial.

Line 438. In figure 8: concentration of sulfate and ammonium seem higher during E – NE air masses; not north west as stated here; a similar pattern to that described for MO-OOA (Line 448).

Authors: The reviewer is correct. “north-westerley” has been changed to “north-easterly”. Furthermore, Figure 8 is now Figure 9.

Line 450: Pattern of LO-OOA is similar to that of HOA Lines 463-466; Section 3.4. Figure 6. There is a clear difference between the ratio LO-OOA/MO-OOA during the eastern and western air masses; any comment on this?

Authors: Although the polar-plot pattern of LO-OOA is similar to that of HOA, the time series of the two factors were not well correlated ($R^2 = 0.30$).

The potential explanation for different contributions of LO-OOA and MO-OOA during the eastern and western air masses has now been reiterated at the end of the next paragraph:

“The higher contribution of MO-OOA compared with LO-OOA from eastern air masses, and vice-versa during western air masses, could be indicative of different OA sources prior to oxidation or due to different photochemical aging between the two directions.”

More measurements, and likely using a higher resolution AMS, would be required to distinguish smaller differences in the MO-OOA and LO-OOA and their differing contributions from the east and west. It is possible that their courses are the same or similar, however they have been kept as separate factors due to their different diurnal and temporal trends and relation to different air masses.

Section 3.5. The measurements of size distribution are limited to the 14-600 nm fractions. The lower size is relatively high for studying the nucleation episodes. Moreover the different air humidity measured for the air clusters defined (sampling was at ambient conditions Line 469-472) may affect these measurements.

Authors: We now indicate that how statements regarding nucleation are constrained to observations > 14 nm. We also indicate that the humidity could shift the measured size distribution to larger sizes:

It should be noted that these size distributions are under ambient conditions without an inlet drier which could shift the size distribution to larger sizes if water is present. The ambient relative humidity for each air mass back trajectory cluster was: Eastern Mediterranean (53%), Central Europe (61%), Atlantic (74%), Western Mediterranean (70%), Mistral (low) (67%) and Mistral (high) (74%). Although the higher temperature inside the PEGASUS mobile laboratory could lower the relative humidity at the sampling point of the SMPS with respect to the ambient relative humidity, this was not measured or logged during the campaign.

Lines 485-487: Has the “nucleation mode ratio” been previously defined? Can you add a reference?

Authors: It has not been previously defined. We have, however, decided to remove this term and simply state it as “the ratio of the particle number concentration between 14 - 25 nm and 14 - 600 nm” or “the ratio of sub-25 nm and sub-600 nm particle number concentrations”.

Line 501: Please, add a reference for shipping emissions

Authors: References have now been included for the statement regarding vanadium and nickel in shipping emissions (Healy et al., 2009; Isakson et al., 2001.):

Healy, R. M., O'Connor, I. P., Hellebust, S., Allanic, A., Sodeau, J. R., & Wenger, J. C.: Characterisation of single particles from in-port ship emissions. *Atmospheric Environment*, 43(40), 6408-6414, 2009.

Isakson, J., Persson, T. A., & Lindgren, E. S.: Identification and assessment of ship emissions and their effects in the harbour of Göteborg, Sweden. *Atmospheric Environment*, 35(21), 3659-3666, 2001

Figure 6. caption: "less oxidized" (LO-OOA) . . .

Authors: The caption for Figure 6 has been changed from “...”less oxidised” (OOA)” to “...”less oxidised” (LO-OOA)”.

1 **Summertime surface PM₁ aerosol composition and size by source region**
2 **at the Lampedusa island in the central Mediterranean Sea**

3 Marc D. Mallet^{1,2,3}, Barbara D'Anna^{2,4}, Aurélie Mème^{2,*}, Maria Chiara Bove^{5,6}, Federico Cassola^{5,7},
4 Giandomenico Pace⁸, Karine Desboeufs¹, Claudia Di Biagio¹, Jean-Francois Doussin¹, Michel
5 Maille¹, Dario Massabò⁵, Jean Sciare⁹, Pascal Zapf¹, Alcide Giorgio di Sarra⁸ and Paola Formenti¹

6 **1. LISA, CNRS UMR7583, Université Paris Est Créteil (UPEC), Université de Paris Diderot (UPD),**
7 **Institut Pierre Simon Laplace (IPSL), Créteil, France**

8 **2. IRCELYON, CNRS UMR 5652, Univ. Lyon1, Lyon, France**

9 **3. Centre National d'Etudes Spatiales (CNES), Toulouse, France**

10 **4. LCE, CNRS UMR 7376, Aix-Marseille Université, Marseille, France**

11 5. Department of Physics & INFN, University of Genoa, Genoa, Italy

12 6. ARPAL Physical Agents and Air Pollution Sector, La Spezia, Italy

13 7. ARPAL CFMI-PC, Genoa, Italy (current affiliation)

14 8. Laboratory for Observations and Analyses of Earth and Climate, ENEA, Rome, Italy

15 9. The Cyprus Institute, Energy, Environment and Water Research Center, Nicosia, Cyprus

16 *now at Bruker

17 For submission to the ChArMex special issue in Atmos. Chem. Phys.

18 **Abstract**

19 Measurements of aerosol composition and size distributions were taken during the summer of
20 2013 at the remote island of Lampedusa in the southern central Mediterranean Sea. These
21 measurements were part of the ChArMEx/ADRIMED (Chemistry and Aerosol Mediterranean
22 Experiment/Aerosol Direct Radiative Forcing on the Mediterranean Climate) framework and
23 took place during the Special Observation Period 1a (SOP-1a) from 11 June until 5 July 2013.

24 From compact time-of-flight aerosol mass spectrometer (cToF-AMS) measurements in the size
25 range below 1 μm in aerodynamic diameter (PM₁), particles were predominately comprised of
26 ammonium and sulphate. On average, ammonium sulphate contributed 63% to the non-
27 refractory PM₁ mass, followed by organics (33%). The organic aerosol was generally very highly
28 oxidised (f_{44} values were typically between 0.25 and 0.26). The contribution of ammonium

29 sulphate was generally higher than organic aerosol in comparison to measurements taken in
30 the western Mediterranean but is consistent with studies ~~undertaken in~~ undertaken in the
31 eastern basin.

32 Source apportionment of organics using a statistical (positive matrix factorisation) model
33 revealed four factors; a hydrocarbon-like organic aerosol (HOA), a methanesulfonic acid related
34 oxygenated organic aerosol (MSA-OOA), a more oxidised oxygenated organic aerosol (MO-OOA)
35 and a less oxidised oxygenated organic aerosol we label (LO-OOA). The MO-OOA was the
36 dominant factor for most of the campaign (53% of the PM₁ OA mass). It was well correlated
37 with SO₄²⁻, highly oxidised, and generally more dominant during easterly air masses originating
38 from the eastern Mediterranean and central Europe. The LO-OOA factor had a very similar
39 composition to the MO-OOA factor, but was more prevalent during westerly winds with air
40 masses originating from the Atlantic Ocean, the western Mediterranean, and in high altitudes
41 over France and Spain from mistral winds. The MSA-OOA factor contributed an average 12% to
42 the PM₁ OA and was more dominant during the mistral winds. The HOA, representing observed
43 primary organic aerosol only contributed 8% of the average PM₁ OA during the campaign.

44 Even though Lampedusa is one of the most remote sites in the Mediterranean, PM₁
45 concentrations ($10 \pm 5 \mu\text{g m}^{-3}$) were comparable to those observed in coastal cities and sites
46 closer to continental Europe. Cleaner conditions corresponded to higher wind speeds.
47 Nucleation and growth of new aerosol particles was observed during periods of northwesterly
48 winds. From a climatology analysis from 1999 until 2012, these periods were much more
49 prevalent during the measurement campaign than during the preceding 13 years. These results
50 support previous findings that highlight the importance of different large-scale synoptic
51 conditions in determining the regional and local aerosol composition and oxidation and also
52 suggest that a non-polluted surface atmosphere over the Mediterranean is rare.

53 1. Introduction

54 The Mediterranean Sea is a unique marine environment, surrounded by mountain ranges and
55 high coastal human populations from Africa, Europe, and Asia, and the two largest deserts in
56 the world; Sahara Desert to the south and Arabian Desert to the East. It presents a diverse and
57 dynamic atmospheric composition and is projected to undergo significant changes in the
58 contribution of freshwater (Sanchez-Gomez et al., 2009), sea surface temperature and
59 precipitation (Mariotti et al., 2015) over the coming decades. The burning of fossil fuels,
60 including shipping pollution, in southern Europe and in large Mediterranean cities, as well as

61 natural sources of aerosol such as sea salt, forest fires and mineral dust provide a highly
62 complex and dynamic mixture of organic and inorganic aerosol and aerosol precursors in this
63 region (Lelieveld et al., 2002). Elevated aerosol loadings over the Mediterranean basin have
64 been attributed to the long-range transport of continental anthropogenic aerosols (Perrone et
65 al., 2013; Sciare et al., 2003; Sciare et al., 2008) and mineral dust transported from Africa
66 (Querol et al., 2009b; Koçak et al., 2007). Boundary layer observations in the eastern
67 Mediterranean have shown significant influence of long-range transported continental pollution
68 from southern and central Europe (Sciare et al., 2003). Furthermore, biomass burning aerosol
69 has frequently been observed over the basin, in particular the dry season in summer when
70 forest fires are more common ([Bougiatioti et al., 2014](#); [Minguillon et al., 2015](#); Pace et al.,
71 2005). Long-ranged plumes from North American fires have also been observed at high
72 altitudes (Formenti et al., 2002; Ortiz-Amezcuca et al., 2014; Brocchi et al., 2018; Ancellet et al.,
73 2016).

74 Previous long-term observations of the chemical composition of aerosol in the Mediterranean
75 have shown that PM₁₀ (particulate mass with aerodynamic diameter less than 10 µm) is
76 composed of secondary ammonium sulphate, primary and secondary organic aerosol from
77 fossil fuels or biogenic origins, with contributions from natural aerosols from the Sahara Desert
78 and sea spray (Bove et al., 2016; Koulouri et al., 2008; Schembari et al., 2014; Calzolari et al.,
79 2015). Mineral and sea salt contributions are significantly less in PM_{2.5} particle fraction (Querol
80 et al., 2009a). Coarse mode particles contribute to the direct radiative effect over the
81 Mediterranean (Perrone and Bergamo, 2011; Meloni et al., 2006) and can also act as
82 condensation sinks for pollutants (Pikridas et al., 2012). Smaller (sub-micron) aerosol particles,
83 while also contributing efficiently to the total aerosol optical depth in this region (Formenti et
84 al., 2018), can also act as efficient cloud condensation nuclei and therefore have influence on
85 cloud formation, lifetime and precipitation (Haywood and Boucher, 2000). Understanding the
86 impact of different natural and anthropogenic sources on the regional composition of the
87 atmosphere is therefore important in our understanding of the influences they have on the
88 climate over the Mediterranean basin and surrounding regions. It is also now widely recognised
89 that aerosols contribute to adverse health effects in humans (World Health Organization, 2016).

90 Consideration of both the local and regional meteorology are needed to characterise the
91 sources and aging of aerosols (Petit et al., 2017). The National Oceanic and Atmospheric
92 Administration's (NOAA) Hybrid Single-Particle Lagrangian Integrated Trajectory model
93 ([HYSPLIT](#); Stein et al., 2015) and other trajectory models (e.g. [FLEXPART](#); (Stohl et al., 2005))
94 have become a widely-used resources in atmospheric studies to compute the backwards or
95 forwards trajectories of air masses at any point on Earth. They can be useful for identifying the

96 possible origin of a particular episode associated with elevated concentrations of aerosols or
97 gases. Combined with in-situ measurements over longer time periods, they provide a more
98 holistic approach in understanding the link between local or region meteorology and
99 atmospheric composition (Schmale et al., 2013; Tadrós et al., 2018; Zhou et al., 2016). This is
100 particularly useful for remote sites where local emissions are insignificant or infrequent.

101 Investigation of the aerosol physical and chemical properties can also help distinguish their
102 respective sources. Positive matrix factorisation (PMF; (Paatero, 1997; Paatero and Tapper,
103 1994)) has proved to be a useful statistical tool in identifying aerosol sources or aging processes
104 of organics. The source apportionment of PM_{2.5} and PM₁₀ over the Mediterranean, from PMF
105 method, has been investigated in recent works and showed a large spatial variability in source
106 contributions (Becagli et al., 2012; 2017; Calzolari et al., 2015; Amato et al., 2016; Diapouli et al.,
107 2017). The PMF approach was also used to study the aerosol source and aging processes by
108 utilising the complex nature of organic aerosol in the Mediterranean (e.g. Hildebrandt et al.,
109 2010, 2011; Bougiatioti et al., 2014; Minguillón et al., 2016; Arndt et al., 2017; Michoud et al.,
110 2017). This approach has become increasingly feasible with the recent widespread
111 implementation of instruments capable of providing real-time, high time- and mass-resolved
112 non-refractory aerosol composition, such as aerosol mass spectrometers (Ulbrich et al., 2009).
113 PMF models have shown to successfully resolve the bulk-composition of sub-micron organic
114 aerosol into the contributions from various primary sources (e.g. biomass burning, fossil fuel
115 burning, cooking aerosol), but can also reveal the contributions and characteristics of secondary
116 (SOA) organic aerosol (Zhang et al., 2011). Factors with similar mass spectra are consistently
117 observed, albeit with different contributions at measuring sites all around the world. The most
118 commonly observed primary organic aerosol factors are hydrocarbon-like OA (HOA), usually
119 from fossil fuel burning as well as biomass burning (BB_{OA}) while SOA can be usually separated
120 into at least two factors, with low-volatility oxygenated OA (LV-OOA) and Semi-Volatile-OOA
121 (SV-OOA) as common examples (Zhang et al., 2011; Crippa et al., 2014). Other types of OOA
122 have also been observed, such as "Marine-OOA" (Schmale et al., 2013), although these are
123 more difficult to resolve given the shift towards more uniform OA composition with aging.

124 The Chemistry-Aerosol Mediterranean Experiment (ChArMEx) collaborative research program,
125 and the Aerosol Direct Radiative Impact on the regional climate in the MEDiterranean region
126 (ADRIMED) project within, were undertaken to investigate the chemistry and climate
127 interactions within the Mediterranean (Mallet et al., 2016). From 11 June until 5 July 2013,
128 numerous experimental setups were deployed across the western and central Mediterranean in
129 what is called the "Special Observation Period - 1a" (SOP-1a), including intensive airborne
130 measurements (Denjean et al., 2016). Two super-sites were set-up at Ersa (at the northern tip

131 of Corsica Island, France) and at the Lampedusa Island (Italy), approximately 1000 km apart on a
132 north-to-south axis in order to characterise surface aerosol chemical, physical and optical
133 properties (Mallet et al., 2016). Numerous secondary sites—were established along the
134 Mediterranean coasts in Spain, Italy and Corsica beyond the SOP-1a have also provided valuable
135 knowledge of the atmospheric composition in the western and central Mediterranean regions
136 (Chrit et al., 2017; Chrit et al., 2018; Becagli et al., 2017).

137 In this paper, we present the first detailed characterisation of PM₁ in the central remote
138 Mediterranean region, using from measurements of size-resolved chemical composition on from
139 the island site of Lampedusa during the ChArMex/ADRIMED SOP-1a. We investigate the source
140 apportionment of PM₁ by considering their chemical and microphysical properties along with
141 ancillary PM₁₀, gaseous and meteorological data, air mass back trajectories as well as
142 complimentary data collected at the Ersa site in Corsica.

143 2. Experimental

144 2.1 Sampling sites

145 Observations took place at the Roberto ~~Serao-Sarao~~ station (<http://www.lampedusa.enea.it/>)
146 on the island of Lampedusa (35°31'5"N, 12°37'51" E, 20 m above sea level) from 11 June to 5
147 July 2013. Ancillary measurements for this study taken at Ersa at the northern tip of Cape
148 Corsica (42°58'5" N, 9°22'49" E, 560 m above sea level), are also considered. The position of the
149 stations is shown in Figure 1.

150 2.2 Instrumentation, measurements and data

151 Instruments at the Lampedusa super-site were housed in the PEGASUS (Portable Gas Field and
152 Aerosol Sampling Unit) station, a portable observatory initiated by LISA, described in Mallet et
153 al. (2016). Relevant to this study, a c-ToF-AMS (Aerodyne Inc., Billerica, USA), was used to
154 measure the size-resolved composition of non-refractory particulate matter below 1 µm (NF-
155 PM₁)(Drewnick et al., 2005). Data was collected with a 3-minute time resolution. The c-ToF-AMS
156 was operated from a certified Total ~~Suspended~~Suspected Particulate (TSP_TPS) sampling head
157 (Rupprecht and Patashnick, Albany, NY, USA) followed by a cyclone impactor cutting off aerosol
158 particles larger than 1 µm in aerodynamic diameter (using a flow rate of 16 lpm). A nafion drier
159 was used, however the relative humidity at the inlet of the c-ToF-AMS was checked throughout
160 the campaign and was always below 55%.

161 | **A particle-into-liquid sampler (Metrohm PILS; Orsini et al. (2003))** was installed on a TSP inlet
162 | and collected samples approximately every hour. Denuders to remove acid/base gases were not
163 | used. Samples were analysed for major **inorganic** and organic anions (F^- , Cl^- , NO_3^- , SO_4^{2-} , PO_4^{3-} ,
164 | $HCOO^-$, CH_3COO^- , $(COO^-)_2$) and cations (Na^+ , NH_4^+ , K^+ , Ca^{2+} , Mg^{2+}) using Ion Chromatography
165 | (Metrohm, model 850 Professional IC) equipped with Metrosep A supp 7 pre-column and
166 | column for anions measurements and Metrosep C4-250 mm pre-column and column for cations
167 | measurements, and a 500 μ L injection loop. The device was operated with a 1-hour time
168 | resolution.

169 | A 13-stage rotating cascade impactor nanoMOUDI (Model 125B, Marple et al., 1991) was used
170 | to measure the size-segregated inorganic elemental composition. The nanoMoudi impactor,
171 | also operated from the TSP inlet, allows the separation of the particles in 13 size classes from 10
172 | nm to 10 μ m diameter with a backup stage. Each sample was collected for 3 days **with a flow**
173 | **rate of 10 lpm** to ensure enough material was collected on each impactor stage. **Filters 47 mm**
174 | **diameter PTFE filters (2 μ m pore size) were used and coated with high quality vacuum grease**
175 | **(Dekati DS-515) to avoid bouncing. They** were then analysed using X-ray fluorescence (PW-2404
176 | spectrometer by PANalytical™) for the particulate elemental concentrations for elements from
177 | Na to Pb as described in Denjean et al. (2016)).

178 | A Scanning Mobility Particle Sizer (SMPS) measured the mobility number size distribution of
179 | aerosols every 3 minutes from 14.6 to 661.2 nm- diameter. The instrument is composed by an
180 | X-ray electrostatic classifier (TSI Inc., model 3080) and a differential Mobility Analyser (DMA; TSI
181 | Inc., model 3081), and a condensation particle counter (CPC; TSI Inc., model 3775) operated at
182 | 1.5/0.3 L min^{-1} aerosol/sheath flows. Data were corrected to take into account the particle
183 | electrical charging probabilities, the CPC counting efficiency, and diffusion losses. Each scan was
184 | recorded with a 5-minute time resolution. A drier was not used on the SMPS inlet and therefore
185 | the size distributions reported are for ambient conditions.

186 | A GRIMM optical particle counter (OPC; GRIMM Inc., model 1.109) was used to measure the
187 | number size distribution over 31 size classes ranging from 0.26 μ m up to 32 μ m (nominal
188 | diameter range assuming the aerosol refractive index of latex spheres in the calibration
189 | protocol). The instrument was operated at a 6-second resolution and data were acquired as 3-
190 | minute averages.

191 | The equivalent black carbon mass concentration (eBC) was determined by the measurement of
192 | light-attenuation at 880 nm performed by a spectral aethalometer (Magee Sci. model AE31)

193 operated at a 2-minute time resolution and equipped with a TSP particle inlet. As the evaluation
194 of eBC is used as a qualitative tracer of pollution, the factory mass conversion factor of 16.6 m^2
195 g^{-1} was applied to the raw measurement of attenuation without further corrections.

196 The meteorological measurements (air pressure, temperature, relative humidity, wind direction
197 and speed and precipitation) were collected by a Vaisala Milos 500 station with a sampling rate
198 of 10 minutes. The wind sensor was installed on a 10-m meteorological tower, while the air
199 temperature and humidity were measured at a height of 2 m.

200 2.3. Data analysis

201 2.3.1. Analysis of the cToF-AMS data

202 The cToF-AMS data set was processed using two different software analysis tools. The first
203 makes use of the widely-used and standard Igor Pro package, Squirrel (version 1.57G). This
204 software processes the raw data and analyzes the unit-mass resolution (UMR) output with a
205 fragmentation table reported in Aiken et al. (2008). The second method uses a cumulative peak
206 fitting analysis and residual analysis and allows the separation of multiple isobaric peaks not
207 taken into account in the traditional analysis of unit mass resolution squirrel data treatment
208 (Muller et al., 2011). Uncertainties in the major chemical species from the cToF-AMS are
209 typically of the order of $\pm 20\%$ (Drewnick et al., 2005).

210 The ionization efficiency (IE) with respect to nitrate anions was calculated every 5-6 days using
211 nebulised 350 nm mobility diameter ammonium nitrate particles (values varied between $1.42 \cdot$
212 10^{-7} and $1.53 \cdot 10^{-7}$). The relative IE (RIE) of ammonium was slightly higher than the default
213 value- and was 4.3 based on the mass spectrum of ammonium nitrate data from IE calibrations.
214 The RIE of sulfate was determined by comparing the theoretical and the measured
215 concentration of a solution of ammonium nitrate and ammonium sulfate and was determined
216 to be the default value of 1.2. For the organic fraction, the default value of 1.4 was used. For
217 each of the major species, a composition dependent collection efficiency was applied as
218 proposed by Middlebrook et al., 2012 and was on average 0.549, very similar to the default
219 value of 0.55.

220

221 The PM_{10} sea salt concentration was estimated in the cToF-AMS by applying a scaling factor of
222 102 to the ion fragment (using the cumulative peak fitting analysis described in Muller et al.,

223 2011) at 57.98 assigned to NaCl as proposed by {Ovadnevaite et al., 2012}. This scaling factor
224 was determined by nebulising monodisperse 300 nm (mobility diameter) NaCl particles into the
225 cToF-AMS and comparing the NaCl⁺ signal to the total mass calculated using the number
226 concentration from a CPC-3010. This calibration was done after the campaign but with similar
227 tuning conditions. The sea salt-SO₄²⁻ (ss-SO₄²⁻) was calculated as 0.252 * 0.3 * [seasalt], where
228 0.252 is the mass ratio of SO₄²⁻ to Na⁺ in sea salt and 0.3 is the mass ratio of Na⁺ to sea salt
229 (Ghahremaninezhad et al., 2016). Given these assumptions, the uncertainty in the seasalt
230 concentrations are likely to be significantly higher than the typical 20%, although the total
231 contribution of seasalt to the PM1 fraction was very small (0.30 μg m⁻³; <4 %).

232
233 Unconstrained positive matrix factorisation was performed on both the unit-mass-resolution
234 spectra of organic aerosol as well as the peak-fitted peaks identified as organics using PMF2
235 v2.08D. This method requires both a matrix for both the organic signals as well as the errors
236 associated with the organics. For the peak-fitted signals, errors for each mass were estimated as

237
$$\Delta I_i = \sqrt{(\alpha^2 t + (\beta + 1))}$$

238 Where I is the ion signal, ΔI is the absolute uncertainty in the ion signal, α and β are constants
239 (1.2 and 0.001, respectively) and t is the instrumental sampling time in seconds (Drewnick et al.,
240 2009; Allan et al., 2003). For both UMR and peak-fitted inputs, up to 8 factors were investigated
241 by altering the seeds from 0 to 50 in increments of 1 and the fpeaks from -1 to 1 in increments
242 of 0.1. Where I is the ion signal, ΔI is the absolute uncertainty in the ion signal, α and β are
243 constants (1.2 and 0.001, respectively) and t is the instrumental sampling time in seconds. For
244 both UMR and peak-fitted inputs, up to 8 factors were investigated by altering the seeds from 0
245 to 50 in increments of 1 and the fpeaks from -1 to 1 in increments of 0.1. This approach is
246 explained in Ulbrich et al. (2009).

247 2.3.2. Air mass back-trajectory calculation and cluster analysis

248 In order to determine potential source regions for aerosols measured at Lampedusa during the
249 SOP-1a, a series of cluster analyses were performed on HYSPLIT air-mass back-trajectories as
250 per the following. Weekly GDAS1-analysis (Global Data Assimilation System; 1° resolution)
251 trajectory files were downloaded from the Air Resources Laboratory (ARL) of the National
252 Oceanic and Atmospheric Administration (NOAA) archive. 144-hour air-mass backwards
253 trajectories were then calculated every hour over the measurement period with ending point at
254 Lampedusa (height of 45 m) using HYSPLIT (Stein et al., 2015) from within the R-package, SplitR.

255 Cluster analyses were then performed on these calculated trajectories, using a trajectory
256 clustering function within the R-package, OpenAir (Carslaw and Ropkins, 2012). Clustering was
257 done using two different methods to calculate the similarity between different trajectories. The
258 first uses the Euclidean distance between the latitude and longitude of each trajectory point (a
259 total of 144 in this case, representing each hour prior to the arrival at the receptor site). The
260 second uses the similarity of the angles of each trajectory from the origin. These two methods
261 are described in Sirois and Bottenheim (1995). For each clustering method, the number of
262 clusters was altered from two up to ten. Six clusters identified using the Euclidean-distance
263 method were selected, producing a realistic separation of the air-mass backwards trajectories
264 and distinct and physically meaningful differences in aerosol composition and size. An
265 additional clustering analysis was also performed over 3 and 6 hour intervals and using 96-hour
266 backwards trajectories and yielded similar results.

267 3. Results and Discussion

268 3.1. Analysis of local and synoptic meteorology

269 The analysis of the hourly resolved 144-h air mass backwards trajectories provides an indication
270 of the origin of the air masses sampled at Lampedusa during the field campaign. Six distinct
271 clusters are identified (Figure 2). Cluster 1, "Eastern Mediterranean", is representative of air
272 masses that circulate around the eastern-central Mediterranean basin before arriving at the
273 Lampedusa site (average altitude of 400 m). Cluster 2, "Central Europe" is representative of air
274 masses arriving from central Europe (average altitude of 800 m). Cluster 3, "Atlantic" is
275 representative of more marine-like air masses that predominately originate over the Atlantic
276 Ocean, pass over the Strait of Gibraltar between Spain and Morocco, and cross the western
277 Mediterranean basin (average altitude of 500 m). Cluster 4, 263 "Western Europe", cluster 5,
278 "Mistral (low)", and cluster 6, "Mistral (high)", all have similar angular trajectories, but are
279 distinguishable by their different wind speeds and altitudes (although the Euclidian method of
280 cluster analysis only considers differences in horizontal distances). The two "Mistral" clusters
281 typically originate over the northern Atlantic Ocean, travel over France at a high altitude before
282 descending over the western Mediterranean and travelling with relatively higher wind speeds
283 towards Lampedusa. The altitude of "Mistral (high)" was, on average, higher than "Mistral
284 (low)" (1400 m and 1000 m, respectively) and also coincided with higher wind speeds at
285 Lampedusa (13 ms^{-1} and 9 ms^{-1} , respectively). In comparison, the trajectories of the "Western
286 Europe" cluster spent much more time circulating at lower altitudes (700 m, on average) over
287 the western Mediterranean basin and, to a certain extent, east of the Lampedusa site.

288 As a complement, the pressure, temperature, relative humidity, wind speed and direction time
289 series recorded at the station are shown in Figure 3. Two main weather regimes are observed:
290 the former characterized by intense (up to nearly 20 m s^{-1}) northwesterly winds, persisting for
291 several days (10-13 June and 22-30 June) and cool temperatures, whereas the latter associated
292 with low-gradient anticyclonic conditions and light winds from the east or southeast, also
293 favouring warmer temperatures (14-21 June and 1-3 July). Temperatures were relatively stable
294 over the sampling period, fluctuating between approximately $18.5 \text{ }^{\circ}\text{C}$ and $28.2 \text{ }^{\circ}\text{C}$. The relative
295 humidity typically ranged from between 70% and 82% with very few and very brief episodes of
296 drier air masses (relative humidity close to or below 50%). The wind speed and direction
297 distributions during the campaign can be compared to the June-July climatology from 1999 to
298 2012 (Figure 4). During the sampling period of this study, the frequency of winds from the
299 north-westerly sectors were nearly double the average when compared to normal conditions,
300 approaching 40% with high winds speeds exceeding 10 m s^{-1} observed during more than 20% of
301 the time.

302 Data of sea level pressure and 1000 mbar meridional wind component composite anomalies
303 obtained from the National Center for Environmental Prediction (NCEP)/National Center for
304 Atmospheric Research (NCAR) Reanalysis (Kalnay et al. 1996) indicate that this particular
305 situation was induced by a “dipolar” pattern, characterized by positive pressure anomalies in
306 the Western Mediterranean and negative ones in the eastern part of the basin (see
307 Supplementary Figure S1). This produced a persisting, stronger than normal gradient over
308 Southern Italy. As a consequence, surface dust episodes typically driven by strong south or
309 southeasterly winds, associated to cyclonic systems moving along northern African coasts, were
310 basically absent during the campaign.

311 3.2 Aerosol composition

312 The dry NR-PM₁ concentrations measured at Lampedusa by the cToF-AMS ranged from 1.9 to
313 $33.4 \mu\text{g m}^{-3}$, with a mean of $10.2 \mu\text{g m}^{-3}$ over the sampling period. Sulphate contributed the
314 most to the measured NR-PM₁ mass ($41\% \pm 9\%$ on average) followed by significant
315 contributions from organics ($31\% \pm 8\%$) and ammonium ($17\% \pm 3\%$). The eBC, nitrate and sea
316 salt (scaled from the NaCl component of m/z 58) contributed $6\% (\pm 4\%)$, $1\% (\pm 0.4\%)$ and 3%
317 ($\pm 2\%$), respectively. Figure 5 shows the total PM₁ concentration (calculated as the sum of the
318 individually measured species), with contribution from each of the species, as well as the
319 calculated PM₁ mass concentration from the SMPS (assuming an average density based on the
320 composition data). There was reasonable agreement (slope = 0.62; R² = 0.67) between the PM₁
321 mass concentration calculated from composition measurements and the SMPS, with

322 discrepancy observed during periods of high sulphate concentrations from the eastern
323 Mediterranean, likely ~~This could be~~ due to a combination of a broader accumulation mode
324 exceeding the upper size limits of the cToF-AMS inlet, differences in sampling line relative
325 humidity, or unaccounted for variations in the collection efficiency. This figure also contains an
326 indication of the air mass origin over the sampling period.

327 ~~During~~ For most of the campaign there was a ~~reasonable~~ agreement (slope = 1; $R^2 = 0.6$)
328 between the $PM_{10} SO_4^{2+}$ (c-ToF-AMS) and the TSP SO_4^{2+} (PILS) concentration, with the
329 exception of periods of high sea salt concentrations when the TSP SO_4^{2+} were significantly
330 higher (slope = 0.5; $R^2 = 0.2$ for TSP Cl^- concentrations $> 10 \mu g m^{-3}$; see Supplementary Figure
331 S2). Supporting measurements of the size-segregated composition from the cascade impactor
332 corroborate this, indicating a higher contribution of elemental sulphur in the coarse mode
333 during periods of higher sea salt (Supplementary Figure S3). These periods corresponded to
334 the "Mistral" air masses, characterised by higher wind speeds and indicated the role of coarse
335 mode sea salt particles in acting as a condensation sink for sulphate species. ~~This indicates that,~~
336 ~~in these circumstances, the sea salt particles acted as a condensation sink for sulphate~~
337 ~~precursors. If these events are frequent, this could have~~ important implications for the
338 radiative properties of these aerosols by altering the scattering properties and, potentially cloud
339 condensation nuclei concentrations and composition.

340 Figure 6 shows the organic mass, split according to different OA factors from the PMF of the OA
341 peaks. From the unconstrained PMF of the UMR and peak-fitted organic mass spectra, the most
342 meaningful solution was found from a 4-factor solution of the UMR analysis (see
343 Supplementary Figures S4 and S5 for the mass reconstruction and time series' residuals). This
344 has resulted in one factor resembling to a primary organic aerosol and three oxygenated
345 organic aerosol (OOA) factors. Herein we label these factors HOA (hydrocarbon-like OA), MO-
346 OOA (more oxidised OOA), LO-OOA (less oxidised OOA) and MSA-OOA (methanesulfonic acid-
347 related OOA).

348 These factors were compared with ambient organic mass spectra listed in the AMS Spectral
349 Database (Ulbrich et al., 2009). The spectra for the OOA factors (see Figure 7) were strongly
350 correlated with each other ($R > 0.97$) and all three were similar to a "continental" OOA factor
351 observed in a ship campaign in the Arctic (Chang et al., 2011), as well as a low-volatility OOA
352 factor identified in Paris (Crippa et al., 2013). Despite the similarities in their mass spectra, they
353 exhibited different diurnal trends (Figure 7) and time series that were associated with different
354 wind directions and air masses and were therefore not recombined into a single OOA factor.

355 The MO-OOA factor was the most dominant factor during the field campaign (~53% of the total
356 OA mass) and was typical of low-volatility/highly oxidized OOA observed in many other
357 studies, in the Mediterranean, with high contributions of m/z 44 ($f_{44} = 0.31$) (e.g. (Hildebrandt et
358 al., 2010; Hildebrandt et al., 2011). This factor was the most prominent during air masses from
359 the Eastern Mediterranean, central Europe and Atlantic (contributing to 71%, 58% and 55% to
360 OA, respectively) and was strongly correlated with ammonium sulphate ($R^2 = 0.68$) over the
361 whole campaign. It also had a distinct diurnal trend, with concentrations increasing during
362 daylight hours, indicative of photochemical processing. The LO-OOA factor was slightly less
363 oxygenated ($f_{44} = 0.26$) and exhibited a different time series ($R^2 = 0.04$), related to different air
364 masses, than the MO-OOA. The less oxygenated OOA factor has also been associated with semi-
365 volatile species and is often labelled as SV-OOA (Jimenez et al., 2009). Despite a distinct diurnal
366 profile similar to previously reported SV-OOA factors (with a peak in the early morning), we
367 refrain from labelling our LO-OOA this way because the mass spectrum was generally much
368 more oxygenated and contained less f_{43} than typically reported SV-OOA (see Figure 98).

369 The MSA-OOA factor contributed approximately 12% of the total OA during the campaign and is
370 likely related to the biogenic emission and processing of dimethyl sulfide (DMS) from
371 phytoplankton in the Mediterranean. This factor was also highly oxygenated ($f_{44} = 0.20$), but
372 contains key peaks related to the fragmentation of MSA from the electron impact of the cToF-
373 AMS. The most prominent of these peaks were m/z 96 (CH_4SO_3^+), 79 (CH_3SO_2^+), 78 (CH_2SO_2^+), 65
374 (HSO_2^+) and 45 (CHS^+). A similar factor was observed at Bird Island in the south Atlantic Ocean
375 (Schmale et al., 2015), albeit without the contribution of significant m/z 44, suggesting a more
376 aged or mixed aerosol during this campaign. A distinct diurnal pattern for the MSA-OOA was
377 not observed.

378 While the MO-OOA, LO-OOA and MSA-OOA factors represent secondary organic aerosol and
379 were the most dominant contribution of OA during the campaign (92% on average), a primary
380 organic aerosol factor was observed and identified here as hydrocarbon-like OA (HOA). The
381 mass spectrum of the HOA factor was characteristic of spectra observed in other studies, with
382 prominent peaks at m/z 95, 91, 83, 81, 71, 69, 57, 55, 43 and 41. Although HOA is typically
383 associated with emissions from incomplete combustion (Zhang et al., 2005), it was not well
384 correlated with other expected tracers such as eBC, CO and NO_x. This HOA was typically
385 associated with south-westerly winds of low speed ($<5 \text{ m s}^{-1}$; see Figure 109) and peaked at
386 approximately 6 am local time each morning. The poor correlation between the HOA factor and
387 eBC could have been due to a variety of local sources with different HOA and eBC emission
388 factors, a mixing of the PMF factor with some small peaks not associated with combustion
389 processes or from regional HOA that has undergone some transport without significant

390 oxidation. The signal fraction of each m/z of the mass spectrum of the HOA factor however had
391 strong correlations ($0.69 < R < 0.89$) with numerous hydrocarbon-like organic aerosol (HOA)
392 factors from other studies (Hersey et al., 2011; Ulbrich et al., 2009; Ng et al., 2011; Lanz et al.,
393 2007; Zhang et al., 2005).

394 3.3 Comparison with other observations around the Mediterranean

395 There are many factors that could influence the composition, the concentration, and oxidation
396 level of different aerosol species over the Mediterranean. These include different aerosol
397 sources which can follow different seasonal or yearly trends (e.g. biogenic emissions) as well as
398 the existing aerosol load and the meteorological conditions that drive transport, dilution and
399 aging processes. ~~Table 1 summarises the recent observations of NR-PM₁ composition from~~
400 ~~measurements in the remote Mediterranean.~~

401 The majority of previous studies of detailed PM₁ aerosol composition have been taken at
402 coastal sites around the Mediterranean (Mohr et al., 2012; Minguillón et al., 2016; Minguillón
403 et al., 2015; Haddad et al., 2013; Bozzetti et al., 2017) which could be expected to observe
404 higher concentrations than at Lampedusa due to proximity to sources (e.g. traffic, fossil fuel
405 use, heating, biomass burning, industrial activities). Aside from Lampedusa and the
406 observations presented in this study, measurements at Finokalia and Cape Corsica could be
407 considered the most remote sites where these measurements have been taken. Similar to the
408 comparison of NR-PM₁ measurements from Europe, North America and east Asia made by
409 Zhang et al., 2007, Figure 8 summarises the recent observations of NR-PM₁ composition from
410 measurements in and around the Mediterranean basin (see Supplementary Tables S1 and S2 for
411 more details that are displayed in Figure 8).

412 The PM₁ mass loading observed at Lampedusa is comparable to most of these other studies
413 performed at both remote marine sites and coastal sites in the Mediterranean (see
414 Supplementary Table S1 for a comparison with coastal urban sites). With the exception of sites
415 in the Eastern Mediterranean, OA was the dominant NR-PM₁ constituent and summertime OA
416 was generally considered mostly secondary, comprised of SV-OOA and LV-OOA with small
417 contributions of HOA. For remote sites, the results are consistent with a predominance of OA in
418 PM₁ fraction in summer. PMF analysis of Q-AMS measurements at the Finokalia remote site in
419 the eastern Mediterranean in the summer of 2008 showed two OOA factors and a distinct lack
420 of HOA (Hildebrandt et al., 2010). A more recent study during the late 2012 summer at Finokalia
421 observed periods influenced by biomass burning, but otherwise also observed mostly
422 oxygenated organic aerosol (Bougiatioti et al., 2014). Measurements undertaken in the western

423 Mediterranean at Cape Corse from 11 June until 6 August 2013, encompassed the sampling
424 period of this study. For the period from 15 July until 5 August, PMF analysis showed 55%, 27%
425 and 13% contributions of organic matter, sulphate and ammonium to non-refractory PM₁
426 (Michoud et al., 2017). Secondary oxygenated VOCs dominated the VOC spectrum during the
427 campaign and were very well correlated with submicron organic aerosol. PMF analysis on the
428 OA revealed a 3-factor solution where SV-OOA and LV-OOA were dominant, contributing by
429 44% and 53%, respectively, with a 4% HOA contribution. From the same measurements but
430 reported over the extended period from 11 June 11 until 5 August 5, there was a higher LV-OOA
431 contribution (62%)(Arndt et al., 2017) which is in agreement with our observations of MO-OOA
432 at Lampedusa. The OA was mostly portioned into MO-OOA and LO-OOA (81%), indicative of
433 well-aged or oxidised secondary organic aerosol from long-range transport of pollutants.
434 ~~Furthermore, the contribution of ammonium sulphate was higher in this study than of all those~~
435 ~~undertaken in the eastern Mediterranean basin, highlighting the role contribution of sulphates~~
436 ~~across the Mediterranean.~~

437 Figure 89 displays the behavior of the f_{44} and f_{43} fragments obtained during the field campaign.
438 f_{44} , a proxy for OA oxidation (Jimenez et al., 2009), is calculated as the ratio of the mass at m/z
439 44 (mostly CO_2^+) to the total OA, while f_{43} , equal to the ratio of m/z 43 (mostly $\text{C}_2\text{H}_3\text{O}^+$) to the
440 total OA, typically represents less aged OA. f_{44} was ~ 0.26 for the majority of the sampling period
441 (Q1: 0.25, Q3: 0.27), while f_{43} was 0.036 (Q1: 0.028, Q3: 0.041). The campaign values are
442 compared to values from the spectra for the four PMF factors and those observed in other field
443 campaigns in the remote Mediterranean. The dotted lines (the so-called "Ng triangle"),
444 encapsulate the f_{44} and f_{43} values of atmospheric OA from a vast number of studies (Ng et al.,
445 2010), with the most aged OA in the top left corner and the most fresh in the bottom right. The
446 high f_{44} values and the dominance of the highly oxygenated MO-OOA and LO-OOA factors show
447 that the organic aerosol was extremely aged compared to other measurements.

448 3.4 Links to meteorology

449 The contribution of the major submicron chemical species and OA sources is further explained
450 in the following by linking the measured and apportioned concentrations to the local
451 meteorology (i.e., wind speed and wind direction) and to the air mass back trajectories to
452 account for the long-range transport of aerosol as well as more distant sources. The bivariate
453 polar plots of these PM₁ species and f_{44} as a function of wind speed and direction are shown in
454 Figure 109.

455 Considering that the sampling site on Lampedusa is on the north east tip of the island, it is
456 evident that the SO_4^{2-} and NH_4^+ were likely a result of north-easterly marine air masses, in

457 agreement with previous results (e.g., Bove et al., 2016). Sea salt concentrations were highest
458 during high north-westerly wind speeds. Higher concentrations of NO_3^- , HOA and some of the
459 periods with elevated eBC concentrations were observed during low speed south-westerly
460 winds, likely a result of the human settlements and activity on the island of Lampedusa
461 (population of ~6000 located to the south west of the sampling site). Besides, the polar plot for
462 eBC showed a patchier pattern, indicative of more local or point sources and the elevated
463 signals were likely due to air masses passing over ship plumes. Although the mass spectra for
464 the LO-OOA and MO-OOA factors were very similar, their bivariate polar plots indicate different
465 sources or photochemical processes. The MO-OOA was more prominent during north-easterly
466 winds, indicating the most aged organics were influenced by air masses from the eastern
467 Mediterranean, either from long-ranged transport ~~or~~ from circulation of closer pollution
468 sources, while the LO-OOA was more dominant during northwesterly wind directions and air
469 masses from over the western Mediterranean. Figure 119 shows the average contribution of
470 each species during different air mass periods (see Supplementary Table S2 for the mean
471 concentrations and standard deviations).

472 The highest concentrations of PM_{10} were observed during "Eastern Mediterranean" and "Central
473 Europe" air mass periods, when significant lifetime over the lower altitude marine environment
474 and/or higher SO_2 emissions allowed the conversion and condensation of sulphate. These aged
475 aerosols are corroborated by the high number concentrations within the accumulation mode
476 during these periods relative to other periods, measured by the SMPS as well as the size-
477 resolved sulphate composition, as discussed in the next section. In contrast to the "Eastern
478 Mediterranean" and "Central Europe" air masses, sulphate concentrations were relatively low
479 during the two "Mistral" air masses. This behavior has been found also in PM_{10} , with elevated
480 values of sea salt aerosol and low non-sea salt sulphate during Mistral events (Becagli et al.,
481 2017). The organic mass concentration was relatively uniform across the periods of different air
482 mass origins, with the exception of the high Mistral winds which yielded OA concentrations
483 approximately half the rest of the campaign and a higher contribution of MSA-OOA in
484 comparison with other periods. The higher contribution of MO-OOA compared with LO-OOA
485 from eastern air masses, and vice-versa during western air masses, could be indicative of
486 different OA sources prior to oxidation or due to different photochemical aging between the
487 two directions.

488 3.5 Aerosol size distributions

489 There are distinctions between the measured PM_{10} size distributions during periods of different
490 air mass origins (Figure 124). It should be noted that these size distributions are under ambient

491 conditions without an inlet drier which could shift the size distribution to larger sizes if water is
492 present. The ambient relative humidity for each air mass back trajectory cluster was: Eastern
493 Mediterranean (53%), Central Europe (61%), Atlantic (74%), Western Mediterranean (70%),
494 Mistral (low) (67%) and Mistral (high) (74%). Although the higher temperature inside the
495 PEGASUS mobile laboratory could lower the relative humidity at the sampling point of the SMPS
496 with respect to the ambient relative humidity, this was not measured or logged during the
497 campaign.

498 Consistent with the higher concentrations of sulphate and ammonium species, the "Eastern
499 Mediterranean" and "Central Europe" had the most pronounced accumulation modes with
500 respect to those from other clusters due to the presence of accumulation mode sulphate (see
501 Supplementary Figure S6 for the size-resolved chemical composition). In contrast, the "Mistral
502 (high)" air masses had very few particles in the accumulation mode and were mostly dominated
503 by nucleation (> 14 nm observations only) and Aitken mode particles, in terms of number. There
504 was only one period of "Mistral (high)" air masses, spanning 38 hours between 09:00 on 24
505 June until 23:00 on 25 June.

506 The most pronounced new particle formation (NPF) events and subsequent growth were
507 observed during the two "Mistral" air masses, particularly between 25 and 27 June. Very high
508 number concentrations in the nucleation mode were also observed in very brief periods during
509 the Atlantic and, to an extent, the "Western Europe" air masses. There was a no trend ($R^2 =$
510 0.03) over the whole campaign between the "nucleation mode ratio" (defined here as the ratio
511 of the particles number concentration between 14 and 25 nm and 14 and 600 nm) and the
512 fraction of CH_3SO_2^+ (a fragment of MSA, measured by the cToF-AMS) to total PM_{10} organics (see
513 Supplementary Figure S7. There was a weak positive trend during periods of the Mistral (high)
514 air mass ($R^2 = 0.39$). No trends were observed between the ratio of sub-25 nm and sub-600 nm
515 particle number concentrations~~nucleation mode ratio~~ and the occurrence of other cToF-AMS
516 fragments such as amines that could be linked with biogenic gas-to-particle conversion.
517 Furthermore, there was a weak negative trend between the nucleation mode ratio~~ratio of sub-~~
518 25 nm and sub-600 nm particle number concentrations and the calculated f_{44} ($R^2 = 0.12$).
519 Without instrumentation to measure the concentration of clusters and smaller aerosols (<14
520 nm) in conjunction with organic vapours over a longer time period, it is difficult to isolate and
521 conclude the origin of these nucleation particles in a general sense and we will limit our analysis
522 to the most pronounced event during the campaign. Figure 132 shows the size distribution over
523 this period as well as SO_2 , eBC and CH_3SO_2^+ , as well as the back trajectory ending at 04:00 UTC
524 on 25 June at Lampedusa. This NPF event occurred during the night and therefore in the
525 absence of photochemistry. There was no discernible increase in eBC or SO_2 during these events

526 and the 3-day cascade impactor sample from 25 until 28 June was characterized by the lowest
527 concentrations of vanadium and nickel (released from heavy oil combustion events due to ship
528 emissions) of the whole campaign. The air mass backwards trajectory during this event was
529 characteristic of the "Mistral (high)" cluster. These are high altitude air masses descended over
530 the Atlantic Ocean before having undergone a hydraulic jump over the southern France region
531 and then a rapid descent over the western Mediterranean basin at high speed before arriving at
532 the Lampedusa site. It is interesting to note that these air masses were anomalous for the
533 typical June/July period at Lampedusa. Although the detected mass of CH_3SO_2^+ is likely due to
534 the condensation of MSA on accumulation mode particles, and considering that the cToF-AMS
535 collection efficiency below ~ 100 nm is poor, the increasing concentration of CH_3SO_2^+ did
536 coincide with the nucleation events during this period, suggesting a possible nucleation and
537 condensation of marine biogenic vapours. Different studies indicate that NPF events may be
538 triggered by atmospheric mixing processes (Kulmala et al., 2004; Hellmuth, 2006; Lauros et al.,
539 2007; Lauros et al., 2011) due to different phenomena like the enhancement of turbulence in
540 elevated layers (Wehner et al., 2010), the break-up of the nocturnal inversion (Stratmann et al.,
541 2003), or the turbulence associated with the nocturnal low-level jet (Siebert et al., 2007). [Night-](#)
542 [time NPF events have also been observed in the Eastern Mediterranean \(Kalivitis et al., 2002\).](#)

543 Furthermore, the intrusion of descending mid-tropospheric air masses in the boundary layer
544 (Pace et al., 2015) has been linked to the occurrence of NPF events and would be consistent
545 with the absence of high concentrations of BC, SO_2 , vanadium and nickel which could be
546 expected from ship emissions ([Healy et al., 2009; Isakson et al., 2001](#)) in the boundary layer
547 over the Mediterranean. Pace et al. (2006) have shown that clean marine aerosol conditions are
548 rare at Lampedusa and generally associated with north-westerly progressively descending
549 trajectories, in agreement with the findings of this study. The relative absence of pre-existing
550 particles acting as a condensation sink favors NPF events as observed during the field campaign.

551 [3.6 Evidence of aging Accumulation of sulphates](#) across the Mediterranean

552 In order to investigate the aging of aerosols across the north-south trajectory of European
553 continental air masses, we compare the average NR- PM_{10} composition measurements at
554 Lampedusa to the concurrent measurements conducted at the Ersa site during summer 2013
555 (Michoud et al., 2016; Arndt et al., 2017). This is shown in Table [12](#).

556 On average, the PM_{10} non-refractory organic mass concentrations at both sites were similar with
557 $\sim 3 \mu\text{g m}^{-3}$. NO_3^- concentrations were relatively small at both sites, but higher at Ersa ($0.28 \mu\text{g m}^{-3}$)
558 than at Lampedusa ($0.09 \mu\text{g m}^{-3}$). Sulphate concentrations were a factor of 3.2 times higher at

559 Lampedusa ($4.5 \mu\text{g m}^{-3}$) than at Ersa ($1.4 \mu\text{g m}^{-3}$) while the ammonium concentrations were a
560 factor of 2.7.

561 | To investigate the possible accumulation of ammonium sulphate during the transport of air
562 masses from Europe, the hourly air-mass back trajectories from Lampedusa were filtered so
563 that only those that passed within $\pm 1^\circ$ latitude and longitude and within ± 200 m altitude of the
564 station height of Ersa (550 m) were selected. These thresholds were chosen arbitrarily since
565 there is no clear distinction in horizontal or vertical distance from the site that would
566 necessarily constitute a representative air mass. This resulted in a total of 192 hourly
567 | observations at the Ersa site over 32 unique air mass backward trajectory runs (see Figure 143).

568 These trajectories were grouped mainly into the "Central Europe" cluster ($n = 12$). The median
569 trajectory duration between the Ersa and Lampedusa sites was 53 hours, with a minimum of 33
570 hours and a maximum of 144 hours (corresponding to the total duration of the HYSPLIT model
571 runs in this case). Those air masses grouped in the "Eastern Mediterranean" cluster had the
572 longest duration time between the sites of 127 hours (while coincident with the Ersa site, these
573 air masses still spent a significant amount of time over the eastern Mediterranean), followed by
574 "Central Europe" (83 hours), "Western Europe" (45 hours) and then the "Mistral (low)" (38
575 hours). In general, between the two sites, there was a 40% enhancement in the organic mass
576 concentration, but an increase in sulphate and ammonium by a factor of 6 and 4, respectively
577 | (Table 12).

578 The accumulation of $(\text{NH}_4)_2\text{SO}_4$ between Ersa and Lampedusa appeared to be dependent on the
579 travel time of the air mass, however different relationships were observed during different air
580 mass clusters. The total sulphate concentration at Lampedusa minus the total sulphate
581 concentration at Ersa for the same air mass and accounting for the travel time as a function of
582 | the travel time is shown in Figure 154.

583 There was a good positive correlation between the difference in sulphate concentrations
584 between the two sites and the travel time for the "Central Europe" and "Eastern
585 Mediterranean" air masses, while weak positive correlations were observed for the "Western
586 Europe" and "Mistral (low)" clusters. It should be pointed out that the travel time was more
587 than 110 hours for the "Eastern Mediterranean" air masses, while it was only between 33 and
588 58 hours for the other three air mass clusters. It is expected that the accumulation of sulphate
589 would increase as the total travel time increases due to the opportunity for SO_2 conversion or
590 from the addition of sulphate from separate air masses which are not accounted for in the
591 HYSPLIT model. Although this relationship is somewhat demonstrated here, there are other
592 | factors that would influence the SO_4^{2+} accumulation. The sulphate concentrations presented

593 here are measured by an ACSM and cToF-AMS at the Ersa and Lampedusa sites, respectively.
594 Both of these instruments have a 100% inlet efficiency between ~100 nm and 800 nm. The
595 conversion of SO₂ to SO₄²⁻ via nucleation and condensation is dependent on the pre-existing
596 aerosol size distribution and condensation sink. Therefore, the use of PM₁ composition can be
597 misleading if the sulphate is condensing on coarse particles. This is demonstrated in
598 Supplementary Figure S2 that shows the size-resolved mass distribution of sulphur and sodium
599 collected every 3 days on multi-stage cascade impactor filters; the relative contribution of
600 sulphur in the PM₁ is higher than that of PM₁₀ in the absence of sodium (a tracer for sea salt).
601 Furthermore, the concentrations of SO₄²⁻ measured by the PILS in the PM₁₀ fraction and cToF-
602 AMS in the PM₁ are approximately equal with low sea salt concentrations (Na⁺ < 2 μgm⁻³), but
603 are nearly a factor of two higher with the PILS for higher sea salt concentrations
604 (Supplementary Figure S3). Furthermore, the emission of SO₂, typically from ships in the
605 Mediterranean, is not necessarily constant over time and is likely not uniformly spread over the
606 basin and within the vertical column (e.g., Becagli et al. (2017)). This could possibly explain the
607 discrepancy between the "accumulationgrowth rate" of sulphate between the Eastern
608 Mediterranean and Central European air mass origins. MoreoverFurthermore, the sample size
609 for this analysis is relatively small and potentially not representative of the general
610 accumulation of SO₄²⁻ but nonetheless they highlight the magnitude of growthaccumulation
611 under different air mass trajectories.

612

613 4. Concluding remarks

614 The measurements carried out at Lampedusa during the ChArMEx/ADRIMED SOP-1a field
615 campaign has provided a unique insight into the surface layer aerosols in the remote Central
616 Mediterranean. Air masses were influenced by transport from the eastern Mediterranean,
617 central Europe, the western Europe, the Atlantic Ocean as well as western Europe. Air mass
618 clustering has been performed to explain observed differences in the aerosol composition and
619 size at Lampedusa.

620 Hourly PM₁ mass ranged from 1.9 to 33.4 μg m⁻³, with an average of 10.2 μg m⁻³. It was
621 composed on average of 41% ± 9% sulphate, 31% ± 8% organics, 17% ± 3% ammonium, 6% ± 4%
622 black carbon, 1% ± 0.4% nitrate and 3% ± 2% sea salt. OA was highly oxidized (f₄₄ ~0.26), and
623 was apportioned to more oxidised oxygenated OA factor (MO-OOA, 53%), less oxidised OOA
624 factor (LO-OOA, 28%), methanesulfonic acid OOA (MSA-OOA, 12%) and to hydrogen-like OA
625 (HOA, 8%). The highest PM₁ mass loadings were observed for air masses from the Eastern
626 Mediterranean and central Europe, mostly due to the accumulation of ammonium and

627 sulphate. Ancillary data from a remote site at the northern point of Cape Corsica in the Western
628 Mediterranean showed increases of SO_4^{2-} concentrations between 2 and $12 \mu\text{g m}^{-3}$ when both
629 sites (Corsica and Lampedusa) were connected. Apart from the dominance of ammonium
630 sulphate on the PM_{10} composition, the mass concentration and sources of OA have shown to be
631 comparable to previous observations at European coastal and remote sites in the
632 Mediterranean. The most pristine air masses, in terms of PM_{10} , were observed during periods
633 with north-westerly winds which originated from the western Mediterranean or at high
634 altitudes over the western European continent. Several nucleation and growth events, as well
635 as large sea salt concentrations were observed during these pristine periods. The largest
636 concentrations of PM_{10} were observed from air masses from central Europe and those that had
637 circulated over the eastern Mediterranean. In contrast to previous measurements of column-
638 integrated aerosol optical properties (Pace et al., 2006; Meloni et al., 2006), we did not observe
639 the presence of dust or biomass burning in the PM_{10} range at the surface.

640 Our results also indicate a clear dichotomy of PM_{10} aerosol composition from different source
641 regions. Air masses from central Europe were characterised by a higher organic fraction than
642 those from the eastern Mediterranean, which were enriched in sulphates. This difference could
643 have potential implications on the optical properties and particularly the cloud condensation
644 nuclei capabilities of those air masses. The relative occurrence of easterly air masses is not
645 evident in the climatological wind roses, nor in a previous study by Pace et al. (2006) that took a
646 climatological approach of the air mass back trajectories arriving at Lampedusa from 2001 -
647 2003. Nonetheless, a re-evaluation of the relative importance and occurrence of different air
648 masses and aerosol properties should be undertaken.

649 *Data availability.* Open-access to the data used for this publication is provided to registered
650 users following the data and publication policy of the ChArMEx program
651 (http://mistrals.sedoo.fr/ChArMEx/Data-Policy/ChArMEx_DataPolicy.pdf). Additional code
652 used in the analysis of data can be obtained upon request from the corresponding or first
653 author. Weekly GDAS1-analysis (Global Data Assimilation System; 1° resolution) trajectory files
654 were downloaded from the Air Resources Laboratory (ARL) of the National Oceanic and
655 Atmospheric Administration (NOAA) archive (<ftp://arlftp.arlhq.noaa.gov/archives/gdas1/>). 144-
656 hour air-mass backwards trajectories were calculated using the R-package, SplitR
657 (<https://github.com/rich-iannone/SplitR>). Cluster analyses were performed on these calculated
658 trajectories, using the R-package, OpenAir (Carslaw and Ropkins, 2012);
659 <https://github.com/cran/openair>). Spectra used for comparison of PMF OA factors from those
660 observed in other studies can be found at
661 <http://cires.colorado.edu/jjimenez-group/AMSSd/>

662 *Author contributions.* PF, BD, KD, JFD, AGdS designed the experiment in Lampedusa, JS designed
663 the experiment in Ersa, with contributions of co-workers. BD, AM, MCB, FC, GP, KD, CDB, JFD,
664 MM, DM, JS, PZ, AGdS and PF performed the experiments. MDM, BD, AM, GP, KD, JS and PF
665 analysed data and all authors contributed to data interpretation. MDM, BD, GP, KD and PF
666 wrote the manuscript with contributions and/or comments from all co-authors.

667 *Competing interests.* The authors declare that they have no conflict of interest.

668 *Special issue statement.* This article is part of the special issue of the Chemistry and Aeosols
669 Mediterranean Experiment (ChArMEx) (ACP/AMT inter-journal SI)". It is not associated with a
670 conference.

671 *Acknowledgements.* This work is part of the ChArMEx project supported by CNRS-INSU, ADEME,
672 Météo-France and CEA in the framework of the multidisciplinary program MISTRALS
673 (Mediterranean Integrated Studies at Regional And Local Scales; <http://mistrals-home.org/>). It
674 has also been supported by the French National Research Agency (ANR) through the ADRIMED
675 program (contract ANR-11-BS56-0006). Measurements at Lampedusa were also supported by
676 the Italian Ministry for University and Research through the NextData and RITMARE Projects.
677 The AERIS national data infrastructure is acknowledged for maintaining the ChArMex database.
678 Observations took place at the Roberto Sarao station (<http://www.lampedusa.enea.it/>).

679

680

681

References

682

683

684 Aiken, A. C., Decarlo, P. F., Kroll, J. H., Worsnop, D. R., Huffman, J. A., Docherty, K. S., Ulbrich, I. M.,
685 Mohr, C., Kimmel, J. R., and Sueper, D.: O/C and OM/OC ratios of primary, secondary, and ambient
686 organic aerosols with high-resolution time-of-flight aerosol mass spectrometry, *Environmental Science &*
687 *Technology*, 42, 4478-4485, 2008.

688 Allan, J. D., Jimenez, J. L., Williams, P. I., Alfarra, M. R., Bower, K. N., Jayne, J. T., Coe, H., and Worsnop,
689 D. R.: Quantitative sampling using an Aerodyne aerosol mass spectrometer 1. Techniques of data
690 interpretation and error analysis, *Journal of Geophysical Research: Atmospheres*, 108, 2003.

691 Ancellet, G., Pelon, J., Totems, J., Chazette, P., Bazureau, A., Sicard, M., Di Iorio, T., Dulac, F., and Mallet,
692 M.: Long-range transport and mixing of aerosol sources during the 2013 North American biomass
693 burning episode: analysis of multiple lidar observations in the western Mediterranean basin,
694 *Atmospheric Chemistry and Physics*, 16, 4725-4742, 2016.

695 Arndt, J., Sciare, J., Mallet, M., Roberts, G. C., Marchand, N., Sartelet, K., Sellegri, K., Dulac, F., Healy, R.
696 M., and Wenger, J. C.: Sources and mixing state of summertime background aerosol in the north-
697 western Mediterranean basin, *Atmospheric Chemistry and Physics*, 17, 6975-7001, 2017.

698 [Becagli, S., Sferlazzo, D. M., Pace, G., di Sarra, A., Bommarito, C., Calzolari, G., Ghedini, C., Lucarelli, F.,](#)
699 [Meloni, D., Monteleone, F., Severi, M., Traversi, R., and Udisti, R.: Evidence for heavy fuel oil combustion](#)
700 [aerosols from chemical analyses at the island of Lampedusa: a possible large role of ships emissions in](#)
701 [the Mediterranean, *Atmos. Chem. Phys.*, 12, 3479-3492, 2012.](#)

702 [Becagli, S., Anello, F., Bommarito, C., Cassola, F., Calzolari, G., Di Iorio, T., di Sarra, A., Gómez-Amo, J.-L.,](#)
703 [Lucarelli, F., Marconi, M., Meloni, D., Monteleone, F., Nava, S., Pace, G., Severi, M., Sferlazzo, D.M.,](#)
704 [Traversi, R., and Udisti, R.: Constraining the ship contribution to the aerosol of the central](#)
705 [Mediterranean, *Atmospheric Chemistry and Physics*, 17, 2067-2084, 2017.](#) [Becagli, S., Anello, F.,](#)
706 [Bommarito, C., Cassola, F., Calzolari, G., Iorio, T. D., Sarra, A. d., Gómez-Amo, J. L., Lucarelli, F., and](#)
707 [Marconi, M.: Constraining the ship contribution to the aerosol of the central Mediterranean,](#)
708 [*Atmospheric Chemistry and Physics*, 17, 2067-2084, 2017.](#)

709 Bougiatioti, A., Stavroulas, I., Kostenidou, E., Zarnpas, P., Theodosi, C., Kouvarakis, G., Canonaco, F.,
710 Prévôt, A., Nenes, A., and Pandis, S.: Processing of biomass-burning aerosol in the eastern
711 Mediterranean during summertime, *Atmospheric Chemistry and Physics*, 14, 4793-4807, 2014.

712 Bove, M., Brotto, P., Calzolari, G., Cassola, F., Cavalli, F., Fermo, P., Hjorth, J., Massabò, D., Nava, S., and
713 Piazzalunga, A.: PM10 source apportionment applying PMF and chemical tracer analysis to ship-borne
714 measurements in the Western Mediterranean, *Atmospheric Environment*, 125, 140-151, 2016.

715 Bozzetti, C., El Haddad, I., Salameh, D., Daellenbach, K. R., Fermo, P., Gonzalez, R., Minguillón, M. C.,
716 Iinuma, Y., Poulain, L., and Elser, M.: Organic aerosol source apportionment by offline-AMS over a full
717 year in Marseille, *Atmospheric Chemistry and Physics*, 17, 8247-8268, 2017.

- 718 Brocchi, V., Krysztofiak, G., Catoire, V., Guth, J., Marécal, V., Zbinden, R., Amraoui, L., Dulac, F., and
719 Ricaud, P.: Intercontinental transport of biomass burning pollutants over the Mediterranean Basin
720 during the summer 2014 ChArMEx-GLAM airborne campaign, *Atmospheric Chemistry and Physics*, 18,
721 6887-6906, 2018.
- 722 [Calzolari, G., Nava, S., Lucarelli, F., Chiari, M., Giannoni, M., Becagli, S., Traversi, R., Marconi, M., Frosini,](#)
723 [D., Severi, M., Udisti, R., di Sarra, A., Pace, G., Meloni, D., Bommarito, C., Monteleone, F., Anello, F., and](#)
724 [Sferlazzo, D. M.: Characterization of PM10 sources in the central Mediterranean, *Atmos. Chem. Phys.*,](#)
725 [15, 13939–13955, 2015.](#) ~~Calzolari, G., Nava, S., Lucarelli, F., Chiari, M., Giannoni, M., Becagli, S., Traversi,~~
726 ~~R., Marconi, M., Frosini, D., and Severi, M.: Characterization of PM10 sources in the central~~
727 ~~Mediterranean, *Atmospheric Chemistry and Physics*, 15, 13939–13955, 2015.~~
- 728 Carslaw, D. C., and Ropkins, K.: Openair—an R package for air quality data analysis, *Environmental*
729 *Modelling & Software*, 27, 52-61, 2012.
- 730 [Chang, R.-W., Leck, C., Graus, M., Müller, M., Paatero, J., Burkhardt, J. F., Stohl, A., Orr, L., Hayden, K., Li,](#)
731 [S.-M., Hansel, A., Tjernström, M., Leaitch, W. R., and Abbatt, J. P. D.: Aerosol composition and sources in](#)
732 [the central Arctic Ocean during ASCOS, *Atmos. Chem. Phys.*, 11, 10619-10636, 2011.](#) ~~Chang, R.-W., Leck,~~
733 ~~C., Graus, M., Müller, M., Paatero, J., Burkhardt, J. F., Stohl, A., Orr, L., Hayden, K., and Li, S.-M.: Aerosol~~
734 ~~composition and sources in the central Arctic Ocean during ASCOS, 2011.~~
- 735 Chrit, M., Sartelet, K., Sciare, J., Pey, J., Marchand, N., Couvidat, F., Sellegri, K., and Beekmann, M.:
736 Modelling organic aerosol concentrations and properties during ChArMEx summer campaigns of 2012
737 and 2013 in the western Mediterranean region, *Atmospheric Chemistry and Physics*, 17, 12509-12531,
738 2017.
- 739 Chrit, M., Sartelet, K., Sciare, J., Pey, J., Nicolas, J. B., Marchand, N., Freney, E., Sellegri, K., Beekmann,
740 M., and Dulac, F.: Aerosol sources in the western Mediterranean during summertime: A model-based
741 approach, *Atmos. Chem. Phys. Discuss.*, [https://doi/. org/10.5194/acp-2017-915](https://doi.org/10.5194/acp-2017-915), in review, 2018.
- 742 Crippa, M., DeCarlo, P., Slowik, J., Mohr, C., Heringa, M., Chirico, R., Poulain, L., Freutel, F., Sciare, J., and
743 Cozic, J.: Wintertime aerosol chemical composition and source apportionment of the organic fraction in
744 the metropolitan area of Paris, *Atmospheric Chemistry and Physics*, 13, 961-981, 2013.
- 745 Crippa, M., Canonaco, F., Lanz, V., Äijälä, M., Allan, J., Carbone, S., Capes, G., Ceburnis, D., Dall'Osto, M.,
746 and Day, D.: Organic aerosol components derived from 25 AMS data sets across Europe using a
747 consistent ME-2 based source apportionment approach, *Atmospheric chemistry and physics*, 14, 6159-
748 6176, 2014.
- 749 Denjean, C., Cassola, F., Mazzino, A., Triquet, S., Chevaillier, S., Grand, N., Bourrienne, T., Momboisse, G.,
750 Sellegri, K., and Schwarzenbock, A.: Size distribution and optical properties of mineral dust aerosols
751 transported in the western Mediterranean, *Atmospheric Chemistry and Physics*, 16, 1081-1104, 2016.
- 752 Drewnick, F., Hings, S. S., DeCarlo, P., Jayne, J. T., Gonin, M., Fuhrer, K., Weimer, S., Jimenez, J. L.,
753 Demerjian, K. L., and Borrmann, S.: A new time-of-flight aerosol mass spectrometer (TOF-AMS)—
754 Instrument description and first field deployment, *Aerosol Science and Technology*, 39, 637-658, 2005.

- 755 Drewnick, F., Hings, S., Alfarra, M., Prevot, A., and Borrmann, S.: Aerosol quantification with the
756 Aerodyne Aerosol Mass Spectrometer: detection limits and ionizer background effects, *Atmos. Meas.*
757 *Tech.*, 2, 33-46, 2009.
- 758 Formenti, P., Boucher, O., Reiner, T., Sprung, D., Andreae, M. O., Wendisch, M., Wex, H., Kindred, D.,
759 Tzortziou, M., and Vasaras, A.: STAAARTE-MED 1998 summer airborne measurements over the Aegean
760 Sea 2. Aerosol scattering and absorption, and radiative calculations, *Journal of Geophysical Research:*
761 *Atmospheres*, 107, 2002.
- 762 Formenti, P., Mbemba Kabuiku, L., Chiapello, I., Ducos, F., Dulac, F., and Tanré, D.: Aerosol optical
763 properties derived from POLDER-3/PARASOL (2005–2013) over the western Mediterranean Sea: I.
764 Quality assessment with AERONET and in situ airborne observations, *Atmos. Meas. Tech. Discuss.*,
765 <https://doi.org/10.5194/amt-2018-251>, 2018.
- 766 Ghahremaninezhad, R., Norman, A.-L., Abbatt, J. P., Levasseur, M., and Thomas, J. L.: Biogenic,
767 anthropogenic and sea salt sulfate size-segregated aerosols in the Arctic summer, *Atmospheric*
768 *Chemistry and Physics*, 16, 5191-5202, 2016.
- 769 Haddad, I. E., D'Anna, B., Temime-Roussel, B., Nicolas, M., Boreave, A., Favez, O., Voisin, D., Sciare, J.,
770 George, C., and Jaffrezo, J.-L.: Towards a better understanding of the origins, chemical composition and
771 aging of oxygenated organic aerosols: case study of a Mediterranean industrialized environment,
772 Marseille, *Atmospheric Chemistry and Physics*, 13, 7875-7894, 2013.
- 773 Haywood, J., and Boucher, O.: Estimates of the direct and indirect radiative forcing due to tropospheric
774 aerosols: A review, *Reviews of geophysics*, 38, 513-543, 2000.
- 775 Healy, R. M., O'Connor, I. P., Hellebust, S., Allan, A., Sodeau, J. R., & Wenger, J. C.:
776 Characterisation of single particles from in-port ship emissions. *Atmospheric*
777 *Environment*, 43(40), 6408-6414, 2009.
- 778 Hellmuth, O.: Columnar modelling of nucleation burst evolution in the convective boundary layer—first
779 results from a feasibility study Part IV: A compilation of previous observations for valuation of simulation
780 results from a columnar modelling study, *Atmospheric Chemistry and Physics*, 6, 4253-4274, 2006.
- 781 Hersey, S., Craven, J., Schilling, K., Metcalf, A., Sorooshian, A., Chan, M., Flagan, R., and Seinfeld, J.: The
782 Pasadena Aerosol Characterization Observatory (PACO): chemical and physical analysis of the Western
783 Los Angeles basin aerosol, *Atmospheric Chemistry and Physics*, 11, 7417-7443, 2011.
- 784 Hildebrandt, L., Engelhart, G., Mohr, C., Kostenidou, E., Lanz, V., Bougiatioti, A., DeCarlo, P., Prevot, A.,
785 Baltensperger, U., and Mihalopoulos, N.: Aged organic aerosol in the Eastern Mediterranean: the
786 Finokalia Aerosol Measurement Experiment–2008, *Atmospheric Chemistry and Physics*, 10, 4167-4186,
787 2010.
- 788 Hildebrandt, L., Kostenidou, E., Lanz, V., Prevot, A., Baltensperger, U., Mihalopoulos, N., Laaksonen, A.,
789 Donahue, N. M., and Pandis, S. N.: Sources and atmospheric processing of organic aerosol in the
790 Mediterranean: insights from aerosol mass spectrometer factor analysis, *Atmospheric Chemistry and*
791 *Physics*, 11, 12499-12515, 2011.

- 792 | **Isakson, J., Persson, T. A., & Lindgren, E. S.: Identification and assessment of ship emissions and their**
793 | **effects in the harbour of Göteborg, Sweden. *Atmospheric Environment*, 35(21), 3659-3666, 2001**
- 794 | Jimenez, J. L., Canagaratna, M., Donahue, N., Prevot, A., Zhang, Q., Kroll, J. H., DeCarlo, P. F., Allan, J. D.,
795 | Coe, H., and Ng, N.: Evolution of organic aerosols in the atmosphere, *Science*, 326, 1525-1529, 2009.
- 796 | Kalivitis, N., Stavroulas, I., Bougiatioti, A., Kouvarakis, G., Gagné, S., Manninen, H. E., Kulmala, M., and
797 | Mihalopoulos, N.: Night-time enhanced atmospheric ion concentrations in the marine boundary layer,
798 | *Atmos. Chem. Phys.*, 12, 3627-3638, <https://doi.org/10.5194/acp-12-3627-2012>, 2012
- 799 | Koçak, M., Mihalopoulos, N., and Kubilay, N.: Chemical composition of the fine and coarse fraction of
800 | aerosols in the northeastern Mediterranean, *Atmospheric Environment*, 41, 7351-7368, 2007.
- 801 | Koulouri, E., Saarikoski, S., Theodosi, C., Markaki, Z., Gerasopoulos, E., Kouvarakis, G., Mäkelä, T.,
802 | Hillamo, R., and Mihalopoulos, N.: Chemical composition and sources of fine and coarse aerosol particles
803 | in the Eastern Mediterranean, *Atmospheric Environment*, 42, 6542-6550, 2008.
- 804 | Kulmala, M., Vehkamäki, H., Petäjä, T., Dal Maso, M., Lauri, A., Kerminen, V.-M., Birmili, W., and
805 | McMurry, P.: Formation and growth rates of ultrafine atmospheric particles: a review of observations,
806 | *Journal of Aerosol Science*, 35, 143-176, 2004.
- 807 | Lanz, V. A., Alfarra, M. R., Baltensperger, U., Buchmann, B., Hueglin, C., Szidat, S., Wehrli, M. N., Wacker,
808 | L., Weimer, S., and Caseiro, A.: Source attribution of submicron organic aerosols during wintertime
809 | inversions by advanced factor analysis of aerosol mass spectra, *Environmental Science & Technology*,
810 | 42, 214-220, 2007.
- 811 | Lauros, J., Nilsson, E., Maso, M. D., and Kulmala, M.: Contribution of mixing in the ABL to new particle
812 | formation based on observations, *Atmospheric Chemistry and Physics*, 7, 4781-4792, 2007.
- 813 | Lauros, J., Sogachev, A., Smolander, S., Vuollekoski, H., Sihto, S.-L., Mammarella, I., Laakso, L., Rannik, Ü.,
814 | and Boy, M.: Particle concentration and flux dynamics in the atmospheric boundary layer as the
815 | indicator of formation mechanism, *Atmospheric Chemistry and Physics*, 11, 5591-5601, 2011.
- 816 | Lelieveld, J., Berresheim, H., Borrmann, S., Crutzen, P., Dentener, F., Fischer, H., Feichter, J., Flatau, P.,
817 | Heland, J., and Holzinger, R.: Global air pollution crossroads over the Mediterranean, *Science*, 298, 794-
818 | 799, 2002.
- 819 | Mallet, M., Dulac, F., Formenti, P., Nabat, P., Sciare, J., Roberts, G., Pelon, J., Ancellet, G., Tanré, D.,
820 | Parol, F., Denjean, C., Brogniez, G., di Sarra, A., Alados-Arboledas, L., Arndt, J., Auriol, F., Blarel, L.,
821 | Bourriane, T., Chazette, P., Chevaillier, S., Claeys, M., D'Anna, B., Derimian, Y., Desboeufs, K., Di Iorio,
822 | T., Doussin, J.-F., Durand, P., Féron, A., Freney, E., Gaimoz, C., Goloub, P., Gómez-Amo, J. L., Granados-
823 | Muñoz, M. J., Grand, N., Hamonou, E., Jankowiak, I., Jeannot, M., Léon, J.-F., Maillé, M., Mailler, S.,
824 | Meloni, D., Menut, L., Momboisse, G., Nicolas, J., Podvin, T., Pont, V., Rea, G., Renard, J.-B., Roblou, L.,
825 | Schepanski, K., Schwarzenboeck, A., Sellegri, K., Sicard, M., Solmon, F., Somot, S., Torres, B., Totems, J.,
826 | Triquet, S., Verdier, N., Verwaerde, C., Waquet, F., Wenger, J., and Zapf, P.: Overview of the Chemistry-
827 | Aerosol Mediterranean Experiment/ Aerosol Direct Radiative Forcing on the Mediterranean Climate

- 828 | [\(ChArMEx/ADRI-MED\) summer 2013 campaign, Atmos. Chem. Phys., 16, 455-504, 2016.](#) Mallet, M.,
829 | Dulac, F., Formenti, P., Nabat, P., Sciare, J., Roberts, G., Pelon, J., Ancellet, G., Tanré, D., and Parol, F.:
830 | [Overview of the chemistry-aerosol Mediterranean experiment/aerosol direct radiative forcing on the](#)
831 | [Mediterranean climate \(ChArMEx/ADRI-MED\) summer 2013 campaign, Atmospheric Chemistry and](#)
832 | [Physics, 16, 455-504, 2016.](#)
- 833 | Mariotti, A., Pan, Y., Zeng, N., and Alessandri, A.: Long-term climate change in the Mediterranean region
834 | in the midst of decadal variability, *Climate Dynamics*, 44, 1437-1456, 2015.
- 835 | Meloni, D., ~~di~~ Sarra, A., Pace, G., and Monteleone, F.: Aerosol optical properties at Lampedusa
836 | (Central Mediterranean). 2. Determination of single scattering albedo at two wavelengths for different
837 | aerosol types, *Atmospheric Chemistry and Physics*, 6, 715-727, 2006.
- 838 | Michoud, V., Sciare, J., Sauvage, S., Dusanter, S., Léonardis, T., Gros, V., Kalogridis, C., Zannoni, N., Féron,
839 | A., and Petit, J.-E.: Organic carbon at a remote site of the western Mediterranean Basin: sources and
840 | chemistry during the ChArMEx SOP2 field experiment, *Atmospheric chemistry and physics*, 17, 8837-
841 | 8865, 2017.
- 842 | [Middlebrook, A., Bahreini, R., Jimenez, J., and Canagaratna, M.: Evaluation of composition-dependent](#)
843 | [collection efficiencies for the aerodyne aerosol mass spectrometer using field data, Atmospheric](#)
844 | [Chemistry and Physics, 46, 258-271, 2012](#)
- 845 | Minguillón, M., Pérez, N., Marchand, N., Bertrand, A., Temime-Roussel, B., Agrios, K., Szidat, S., van
846 | Drooge, B., Sylvestre, A., and Alastuey, A.: Secondary organic aerosol origin in an urban environment:
847 | influence of biogenic and fuel combustion precursors, *Faraday Discuss*, 189, 337-359, 2016.
- 848 | Minguillón, M. C., Ripoll, A., Pérez, N., Prévôt, A., Canonaco, F., Querol, X., and Alastuey, A.: Chemical
849 | characterization of submicron regional background aerosols in the western Mediterranean using an
850 | Aerosol Chemical Speciation Monitor, *Atmospheric Chemistry and Physics*, 15, 6379-6391, 2015.
- 851 | Mohr, C., DeCarlo, P., Heringa, M., Chirico, R., Slowik, J., Richter, R., Reche, C., Alastuey, A., Querol, X.,
852 | and Seco, R.: Identification and quantification of organic aerosol from cooking and other sources in
853 | Barcelona using aerosol mass spectrometer data, *Atmospheric Chemistry and Physics*, 12, 1649-1665,
854 | 2012.
- 855 | Muller, M., George, C., and D'Anna, B.: Enhanced spectral analysis of C-TOF Aerosol Mass Spectrometer
856 | data: iterative residual analysis and cumulative peak fitting, [INTERNATIONAL JOURNAL OF MASS-](#)
857 | [SPECTROMETRY](#)[International Journal of Mass Spectrometry](#), 306, 1-8, 2011.
- 858 | Ng, N., Canagaratna, M., Zhang, Q., Jimenez, J., Tian, J., Ulbrich, I., Kroll, J., Docherty, K., Chhabra, P., and
859 | Bahreini, R.: Organic aerosol components observed in Northern Hemispheric datasets from Aerosol
860 | Mass Spectrometry, *Atmospheric Chemistry and Physics*, 10, 4625-4641, 2010.
- 861 | Ng, N., Canagaratna, M., Jimenez, J., Chhabra, P., Seinfeld, J., and Worsnop, D.: Changes in organic
862 | aerosol composition with aging inferred from aerosol mass spectra, *Atmospheric Chemistry and Physics*,
863 | 11, 6465-6474, 2011.

- 864 Orsini, D. A., Ma, Y., Sullivan, A., Sierau, B., Baumann, K., and Weber, R. J.: Refinements to the particle-
865 into-liquid sampler (PILS) for ground and airborne measurements of water soluble aerosol composition,
866 Atmospheric Environment, 37, 1243-1259, 2003.
- 867 Ortiz-Amezcuca, P., Guerrero-Rascado, J., Granados-Muñoz, M., Bravo-Aranda, J., and Alados-Arboledas,
868 L.: Characterization of atmospheric aerosols for a long range transport of biomass burning particles from
869 canadian forest fires over the southern iberian peninsula in July 2013, Optica Pura y Aplicada, 47, 43-49,
870 2014.
- 871 Ovadnevaite, J., Ceburnis, D., Canagaratna, M., Berresheim, H., Bialek, J., Martucci, G., Worsnop, D. R.,
872 and O'Dowd, C.: On the effect of wind speed on submicron sea salt mass concentrations and source
873 fluxes, Journal of Geophysical Research: Atmospheres (1984–2012), 117, 2012.
- 874 Paatero, P., and Tapper, U.: Positive matrix factorization: A non-negative factor model with optimal
875 utilization of error estimates of data values, Environmetrics, 5, 111-126, 1994.
- 876 Paatero, P.: Least squares formulation of robust non-negative factor analysis, Chemometrics and
877 [i](#)ntelligent [L](#)aboratory [S](#)ystems, 37, 23-35, 1997.
- 878 Pace, G., Meloni, D., and [d](#)i Sarra, A.: Forest fire aerosol over the Mediterranean basin during summer
879 2003, Journal of Geophysical Research: Atmospheres, 110, 2005.
- 880 [Pace, G., Meloni, D., and di Sarra, A.: Forest fire aerosol over the Mediterranean basin during summer](#)
881 [2003, Journal of Geophysical Research: Atmospheres, 110, D21202, doi:10.1029/2005JD005986, 2005.](#)
- 882 [Pace, G., di Sarra, A., Meloni, D., Piacentino, S., and Chamard, P.: Aerosol optical properties at](#)
883 [Lampedusa \(Central Mediterranean\). 1. Influence of transport and identification of different aerosol](#)
884 [types, Atmospheric Chemistry and Physics, 6, 697-713, 2006.](#)~~[Pace, G., Sarra, A. d., Meloni, D., Piacentino,](#)~~
885 ~~[S., and Chamard, P.: Aerosol optical properties at Lampedusa \(Central Mediterranean\). 1. Influence of](#)~~
886 ~~[transport and identification of different aerosol types, Atmospheric Chemistry and Physics, 6, 697-713,](#)~~
887 ~~[2006.](#)~~
- 888 ~~[Pace, G., Junkermann, W., Vitali, L., Di Sarra, A., Meloni, D., Cacciani, M., Cremona, G., Iannarelli, A. M.,](#)~~
889 ~~[and Zanini, G.: On the complexity of the boundary layer structure and aerosol vertical distribution in the](#)~~
890 ~~[coastal Mediterranean regions: a case study, Tellus-B: Chemical and Physical Meteorology, 67, 27721,](#)~~
891 ~~[2015.](#)~~
- 892 Perrone, M., and Bergamo, A.: Direct radiative forcing during Sahara dust intrusions at a site in the
893 Central Mediterranean: Anthropogenic particle contribution, Atmospheric [R](#)esearch, 101, 783-798,
894 2011.
- 895 Perrone, M., Becagli, S., Orza, J. G., Vecchi, R., Dinoi, A., Udisti, R., and Cabello, M.: The impact of long-
896 range-transport on PM1 and PM2. 5 at a Central Mediterranean site, Atmospheric environment, 71,
897 176-186, 2013.
- 898 Petit, J.-E., Favez, O., Albinet, A., and Canonaco, F.: A user-friendly tool for comprehensive evaluation of
899 the geographical origins of atmospheric pollution: Wind and trajectory analyses, Environmental

900 Modelling & Software, 88, 183-187, 2017.

901 Pikridas, M., Riipinen, I., Hildebrandt, L., Kostenidou, E., Manninen, H., Mihalopoulos, N., Kalivitis, N.,
902 Burkhardt, J. F., Stohl, A., and Kulmala, M.: New particle formation at a remote site in the eastern
903 Mediterranean, *Journal of Geophysical Research: Atmospheres*, 117, 2012.

904 Querol, X., Alastuey, A., Pey, J., Cusack, M., Pérez, N., Mihalopoulos, N., Theodosi, C., Gerasopoulos, E.,
905 Kubilay, N., and Koçak, M.: Variability in regional background aerosols within the Mediterranean,
906 *Atmospheric Chemistry and Physics*, 9, 4575-4591, 2009a.

907 Querol, X., Pey, J., Pandolfi, M., Alastuey, A., Cusack, M., Pérez, N., Moreno, T., Viana, M., Mihalopoulos,
908 N., and Kallos, G.: African dust contributions to mean ambient PM₁₀ mass-levels across the
909 Mediterranean Basin, *Atmospheric Environment*, 43, 4266-4277, 2009b.

910 Rinaldi, M., Gilardoni, S., Paglione, M., Sandrini, S., Decesari, S., Zanca, N., Marinoni, A., Cristofanelli, P.,
911 Bonasoni, P., and Ielpo, P.: Physico-chemical characterization of Mediterranean background aerosol at
912 the Capogranitola observatory (Sicily), *EGU General Assembly Conference Abstracts*, 2017, 3161.

913 Sanchez-Gomez, E., Somot, S., and Mariotti, A.: Future changes in the Mediterranean water budget
914 projected by an ensemble of regional climate models, *Geophysical Research Letters*, 36, 2009.

915 Schembari, C., Bove, M., Cuccia, E., Cavalli, F., Hjorth, J., Massabò, D., Nava, S., Udisti, R., and Prati, P.:
916 Source apportionment of PM₁₀ in the Western Mediterranean based on observations from a cruise
917 ship, *Atmospheric environment*, 98, 510-518, 2014.

918 Schmale, J., Schneider, J., Nemitz, E., Tang, Y., Dragosits, U., Blackall, T., Trathan, P., Phillips, G., Sutton,
919 M., and Braban, C.: Sub-Antarctic marine aerosol: dominant contributions from biogenic sources,
920 *Atmospheric Chemistry and Physics*, 13, 8669-8694, 2013.

921 Sciare, J., Bardouki, H., Moulin, C., and Mihalopoulos, N.: Aerosol sources and their contribution to the
922 chemical composition of aerosols in the Eastern Mediterranean Sea during summertime, *Atmospheric
923 Chemistry and Physics*, 3, 291-302, 2003.

924 Sciare, J., Oikonomou, K., Favez, O., Liakakou, E., Markaki, Z., Cachier, H., and Mihalopoulos, N.: Long-
925 term measurements of carbonaceous aerosols in the Eastern Mediterranean: evidence of long-range
926 transport of biomass burning, *Atmospheric Chemistry and Physics*, 8, 5551-5563, 2008.

927 Siebert, H., Wehner, B., Hellmuth, O., Stratmann, F., Boy, M., and Kulmala, M.: New-particle formation
928 in connection with a nocturnal low-level jet: Observations and modeling results, *Geophysical Research
929 Letters*, 34, 2007.

930 Sirois, A., and Bottenheim, J. W.: Use of backward trajectories to interpret the 5-year record of PAN and
931 O₃ ambient air concentrations at Kejimikujik National Park, Nova Scotia, *Journal of Geophysical
932 Research: Atmospheres*, 100, 2867-2881, 1995.

933 Stein, A., Draxler, R. R., Rolph, G. D., Stunder, B. J., Cohen, M., and Ngan, F.: NOAA's HYSPLIT
934 atmospheric transport and dispersion modeling system, *Bulletin of the American Meteorological*

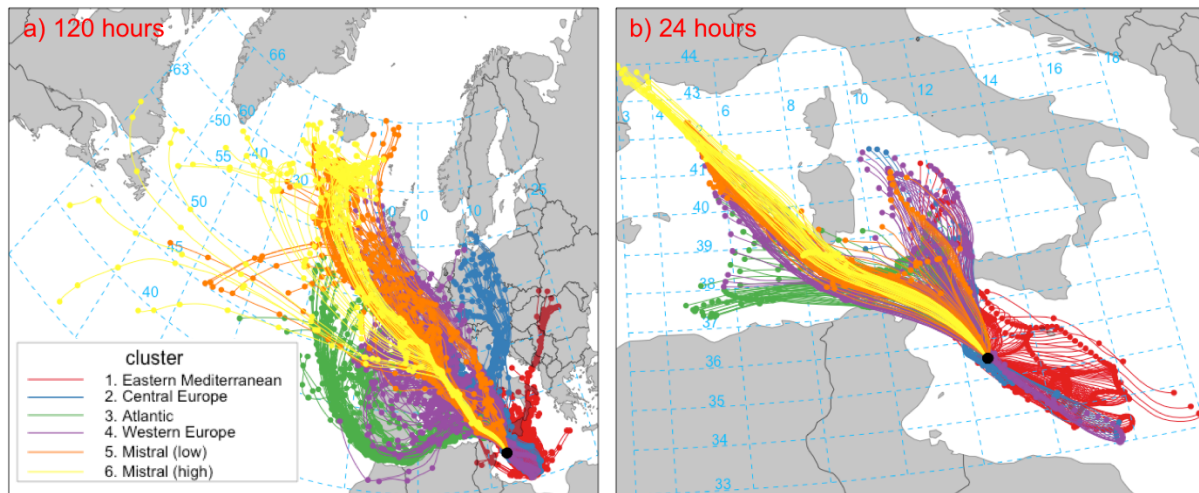
- 935 Society, 96, 2059-2077, 2015.
- 936 Stohl, A., Forster, C., Frank, A., Seibert, P., and Wotawa, G.: The Lagrangian particle dispersion model
937 FLEXPART version 6.2, Atmospheric Chemistry and Physics, 5, 2461-2474, 2005.
- 938 Stratmann, F., Siebert, H., Spindler, G., Wehner, B., Althausen, D., Heintzenberg, J., Hellmuth, O., Rinke,
939 R., Schmieder, U., and Seidel, C.: New-particle formation events in a continental boundary layer: first
940 results from the SATURN experiment, Atmospheric Chemistry and Physics, 3, 1445-1459, 2003.
- 941 Tadros, C. V., Crawford, J., Treble, P. C., Baker, A., Cohen, D. D., Atanacio, A. J., Hankin, S., and Roach, R.:
942 Chemical characterisation and source identification of atmospheric aerosols in the Snowy Mountains,
943 south-eastern Australia, Science of The Total Environment, 630, 432-443, 2018.
- 944 Ulbrich, I., Canagaratna, M., Zhang, Q., Worsnop, D., and Jimenez, J.: Interpretation of organic
945 components from Positive Matrix Factorization of aerosol mass spectrometric data, Atmospheric
946 Chemistry and Physics, 9, 2891-2918, 2009.
- 947 Wehner, B., Siebert, H., Ansmann, A., Ditas, F., Seifert, P., Stratmann, F., Wiedensohler, A., Apituley, A.,
948 Shaw, R., and Manninen, H.: Observations of turbulence-induced new particle formation in the residual
949 layer, Atmospheric chemistry and physics, 10, 4319-4330, 2010.
- 950 **World Health Organization.: Ambient air pollution: A global assessment of exposure and**
951 **burden of disease, 2016.**
952
- 953 Zhang, H., Surratt, J., Lin, Y., Bapat, J., and Kamens, R.: Effect of relative humidity on SOA formation from
954 isoprene/NO photooxidation: enhancement of 2-methylglyceric acid and its corresponding oligoesters
955 under dry conditions, Atmospheric Chemistry and Physics, 11, 6411-6424, 2011.
- 956 Zhang, Q., Worsnop, D., Canagaratna, M., and Jimenez, J. L.: Hydrocarbon-like and oxygenated organic
957 aerosols in Pittsburgh: insights into sources and processes of organic aerosols, Atmospheric Chemistry
958 and Physics, 5, 3289-3311, 2005.
- 959 [Zhang, Q., Jimenez, J. L., Canagaratna, M. R., Allan, J. D., Coe, H., Ulbrich, I., Alfarra, M. R., Takami, A.,](#)
960 [Middlebrook, A. M., Sun, Y. L., Dzepina, K., Dunlea, E., Docherty, K., DeCarlo, P. F., Salcedo, D., Onasch,](#)
961 [T., Jayne, J. T., Miyoshi, T., Shimojo, A., Hatakeyama, S., Takegawa, N., Kondo, Y., Schneider, J.,](#)
962 [Drewnck, F., Borrmann, S., Weimer, S., Demerjian, K., Williams, P., Bower, K., Bahreini, R., Cottrell, L.,](#)
963 [Griffin, R. J., Rautiainen, J., Sun, J. Y., Zhang, Y. M., and Worsnop, D. R.: Ubiquity and dominance of](#)
964 [oxygenated species in organic aerosols in anthropogenically-influenced Northern Hemisphere](#)
965 [midlatitudes, Geophys. Res. Lett., 34, L13801, doi:10.1029/2007GL029979, 2007.](#)
- 966 Zhou, S., Collier, S., Xu, J., Mei, F., Wang, J., Lee, Y. N., Sedlacek, A. J., Springston, S. R., Sun, Y., and
967 Zhang, Q.: Influences of upwind emission sources and atmospheric processing on aerosol chemistry and
968 properties at a rural location in the Northeastern US, Journal of Geophysical Research: Atmospheres,
969 121, 6049-6065, 2016.
970
971



972

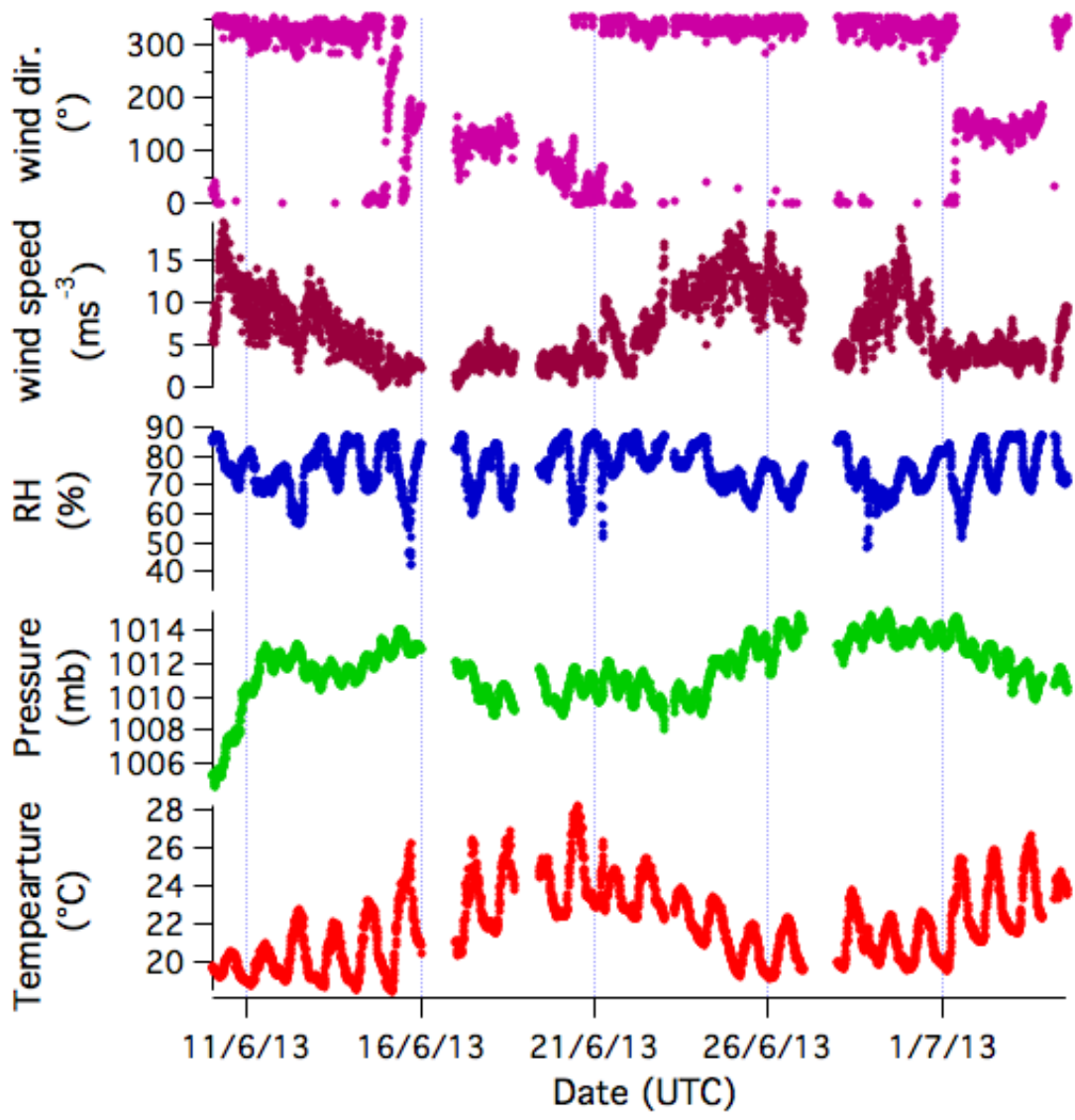
973 *Figure 1 The Mediterranean basin. The two sites considered in this study, Lampedusa and Ersar, are indicated with*
 974 *white dots. Image is courtesy of Google Earth.*

975



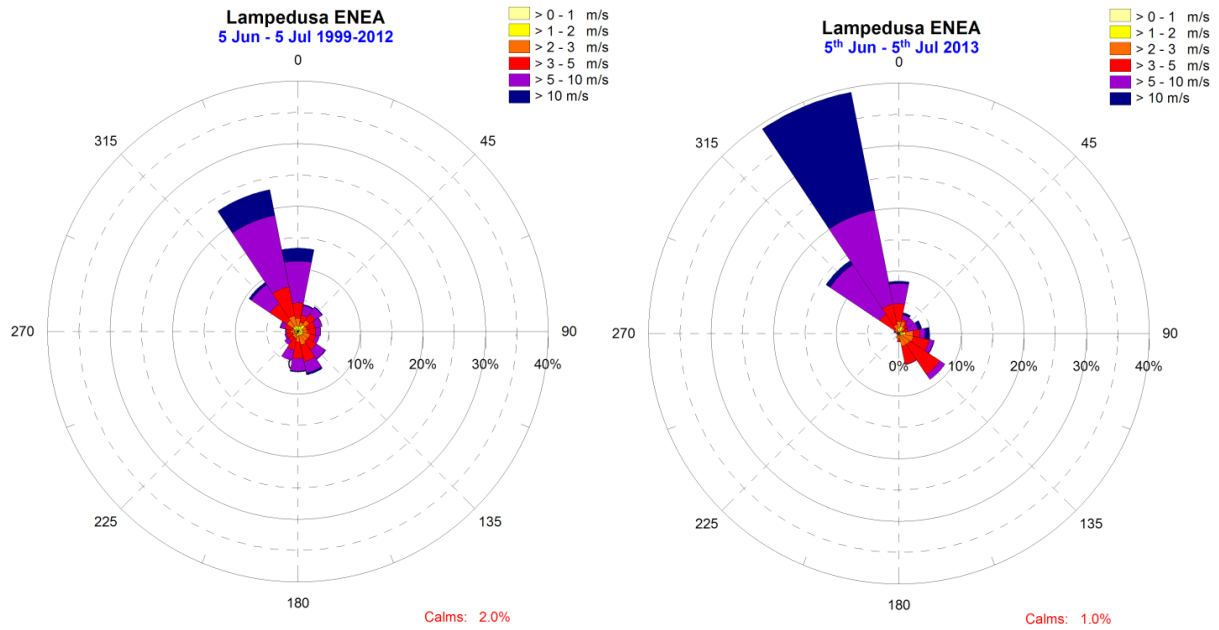
976

977 *Figure 2 a) Hourly 144-hour (6 days) backwards trajectories from Lampedusa from 10 June 2013 until 5 July 2013,*
 978 *cut off at 120 hours (5 days). Colours represent the assigned cluster. B) The same as a) but cut off at 24-hour.*

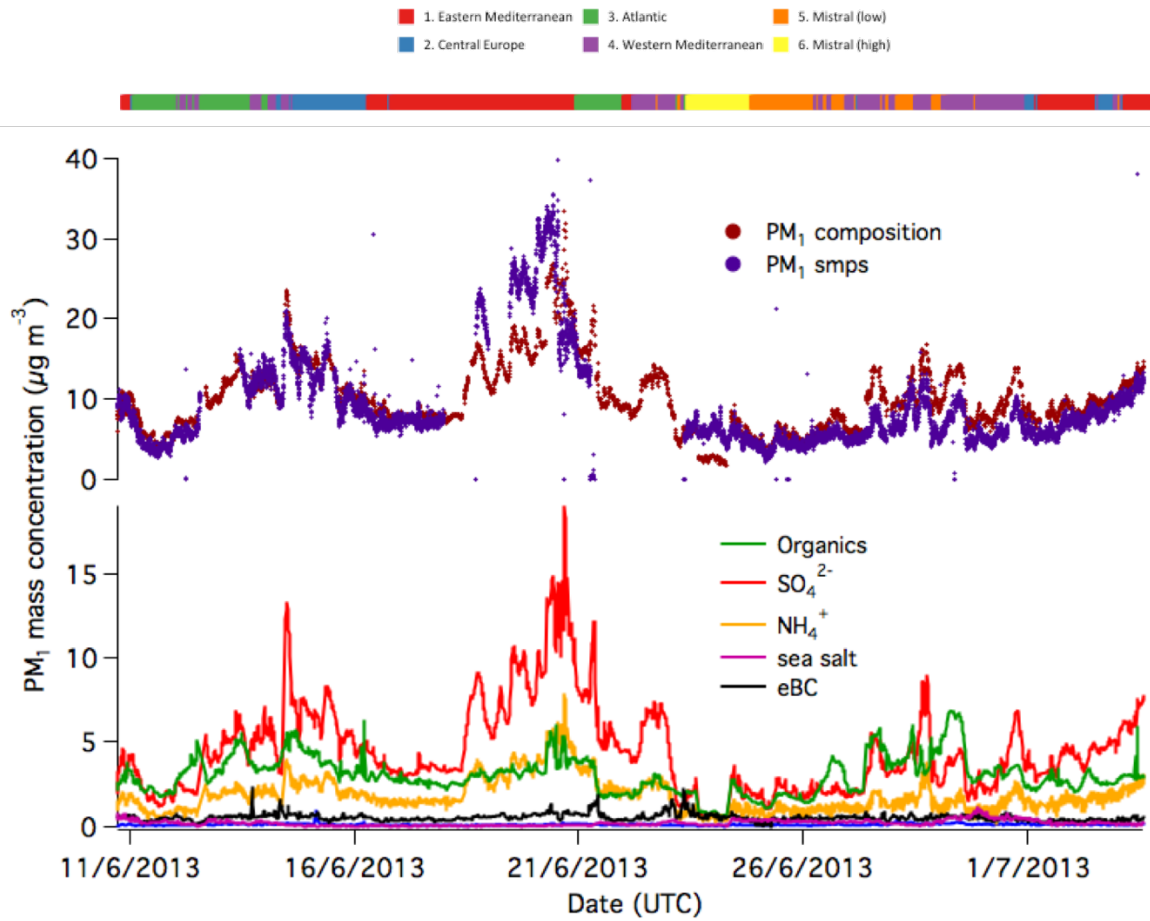


979
 980
 981
 982

Figure 3 Meteorological conditions (wind direction and speed, relative humidity, pressure and temperature) measured at the Lampedusa site during SOP-1a.

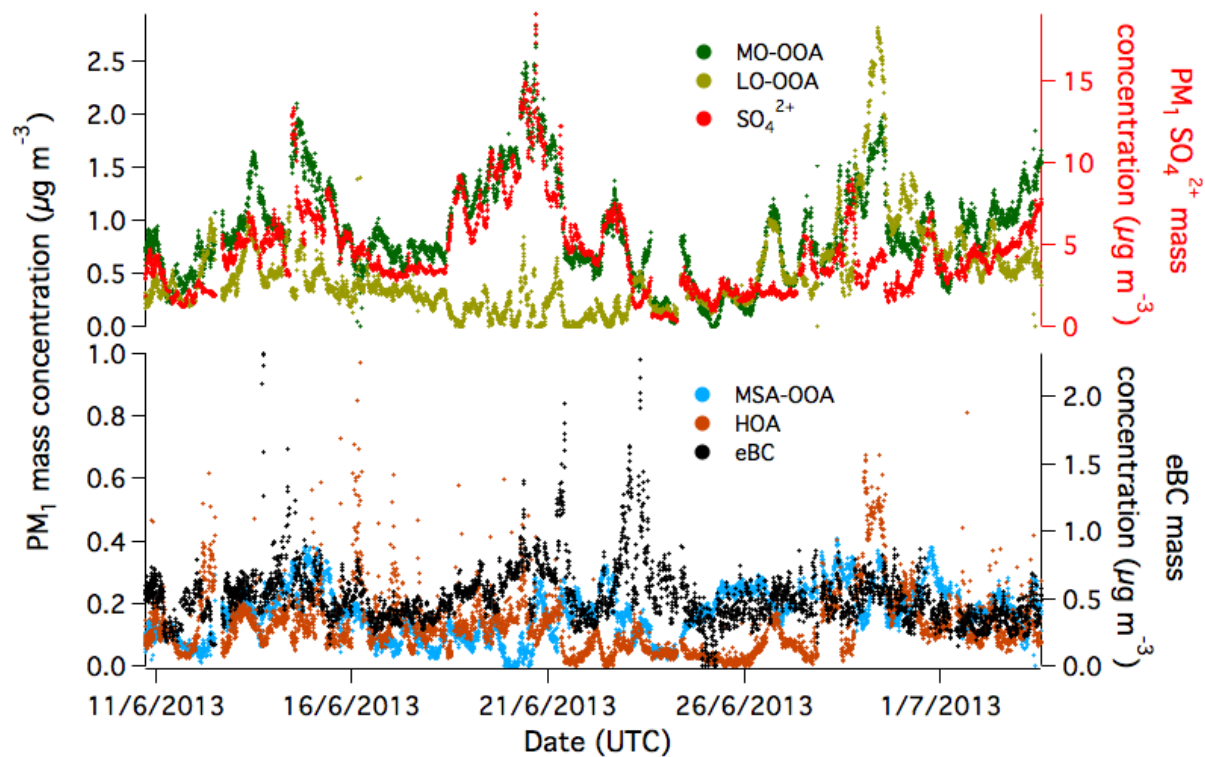


983
 984 *Figure 4 Wind speed and direction at Lampedusa during the period from 5 June until 5 July during the years from*
 985 *1999 - 2012 (left) and during this campaign (right).*

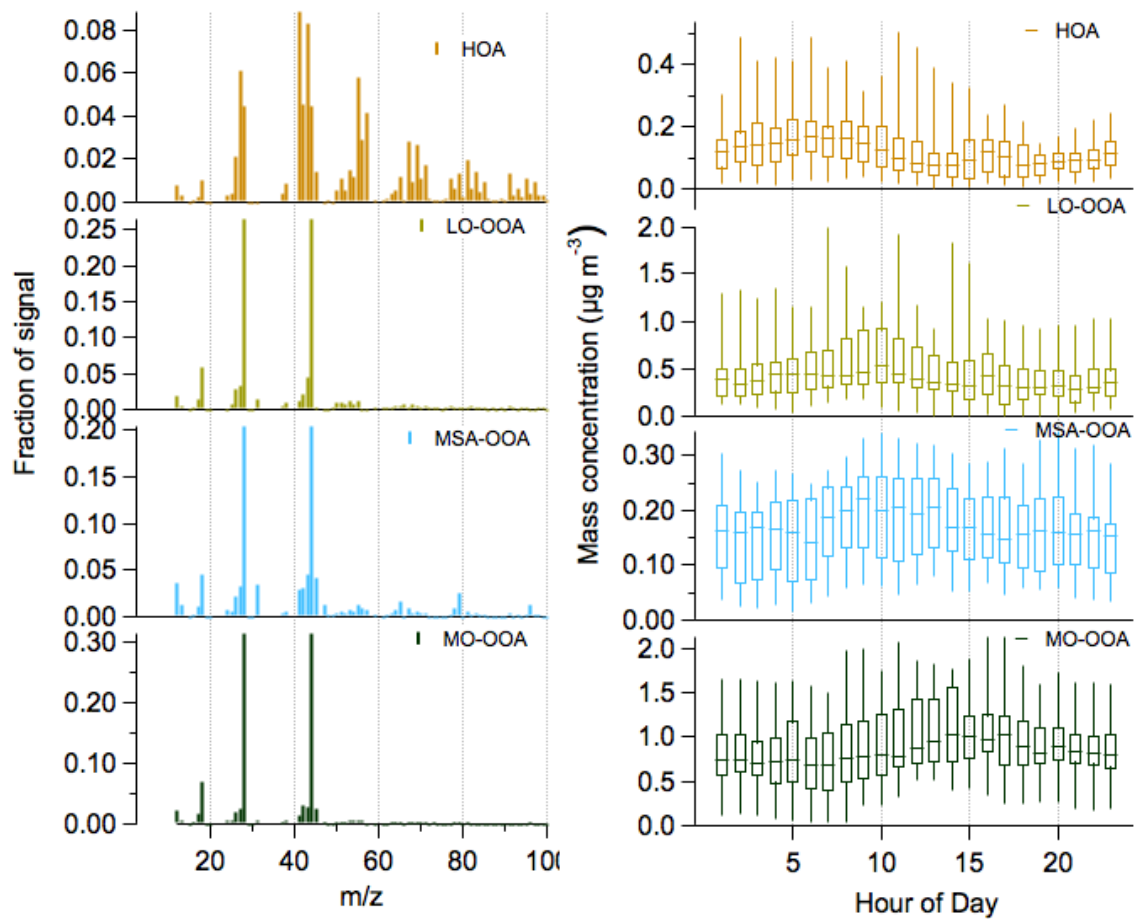


986
987
988

Figure 5 The time series of PM₁ mass concentration, coloured by the relative contribution from each species. The top bar is coloured according to the air mass origin.

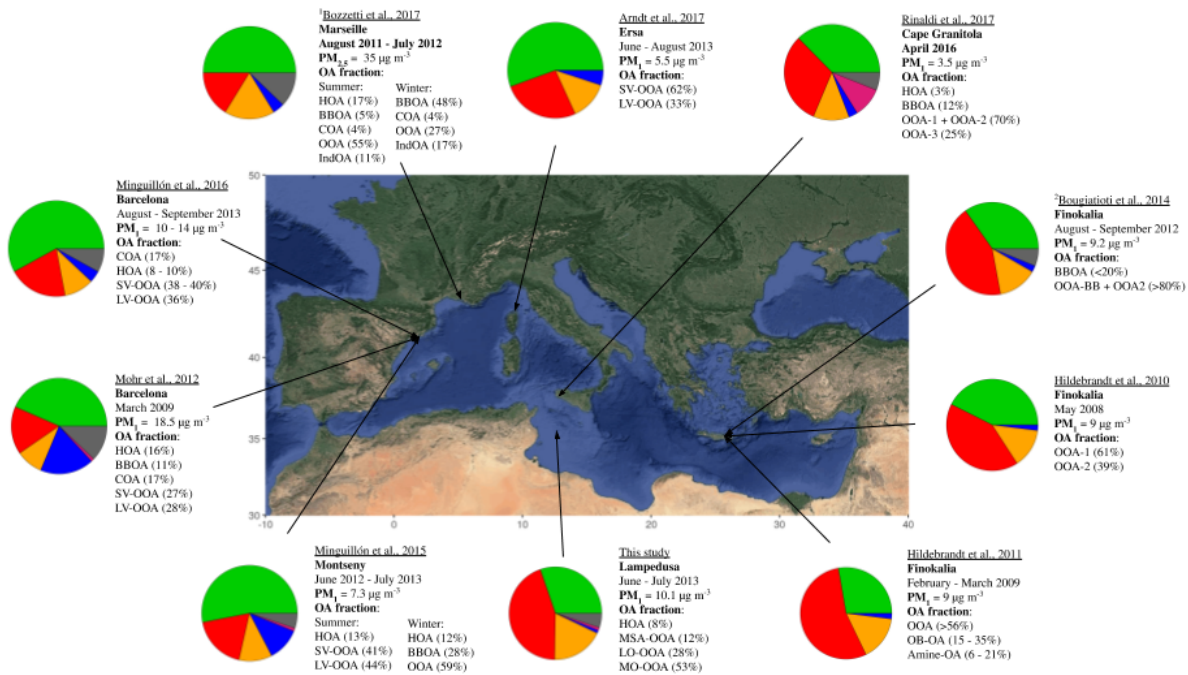


989
 990 *Figure 6 The time series of the PM₁ "more oxidised" OOA (MO-OOA), "less oxidised" (LO-OOA) and sulphate (top*
 991 *panel) and methanesulfonic acid-related OOA (MSA-OOA), hydrocarbon-like OA (HOA) and eBC (bottom panel).*



992
 993 *Figure 7 The mass spectra for the 4 PMF factors (HOA: hydrocarbon-like organic aerosol, LO-OOA: less oxidised*
 994 *OOA, MO-OOA: more oxidised OOA, MSA-OOA: methanesulfonic acid-related OOA) retrieved from the PMF*
 995 *analysis of unit-mass resolution data.*

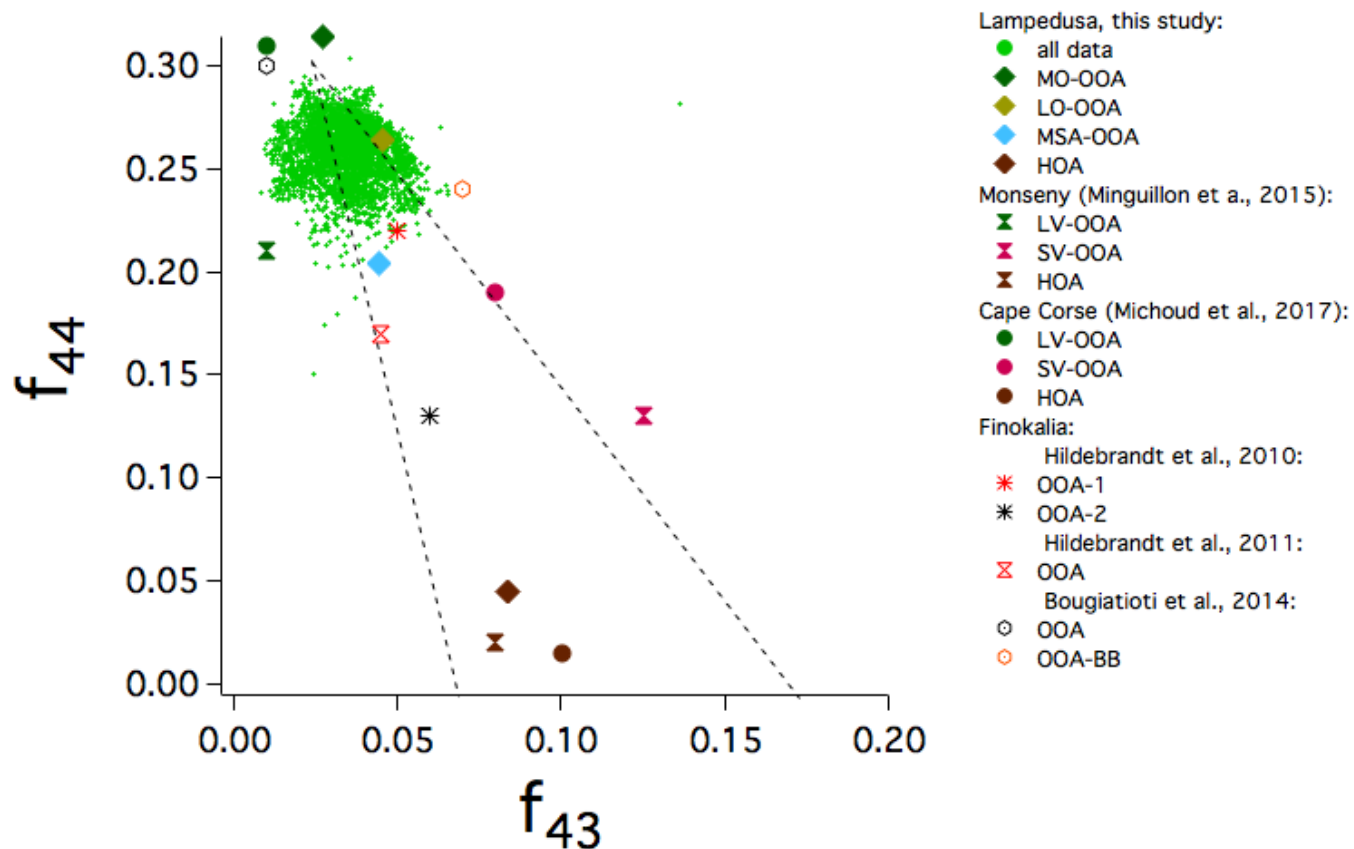
996



997 **Table 1** Figure 8. A summary of studies that have investigated NR-PM₁ composition (including PMF of OA) on islands
 998 around within the Mediterranean basin and at coastal sites surrounding the basin. Only studies that have investigated
 999 PMF-based OA source apportionment are reported. Pie charts display the average concentration during each study
 1000 where green corresponds to organics, red to sulphates, orange to ammonium, blue to nitrate, pink to either chlorides
 1001 or sea salt and black to elemental or black carbon. The OA fraction acronyms correspond to the following:
 1002 HOA: Hydrocarbon-like Organic Aerosol, SV-OOA: Semi-volatile oxygenated Organic Aerosol, LV-OOA: Low-
 1003 volatility oxygenated Organic Aerosol, BBOA: Biomass burning Organic Aerosol, COA: Cooking Organic Aerosol,
 1004 OOA: Oxygenated Organic Aerosol, F4: "Factor -4" (unidentified PMF factor), IndOA: Industry-related Organic
 1005 Aerosol, OB-OA: "Olive-branch Organic Aerosol. See Supplementary Tables S1 and S2 for further details about the
 1006 sampling locations, instruments used and pie chart values. PMF factors in bold indicate secondary organic aerosol.
 1007 After the results of this study, observations are ordered according to longitude (west to east). ¹This study collected on
 1008 PM_{2.5} filters and nebulised into an HR-ToF-AMS. ²Excludes fire-periods.

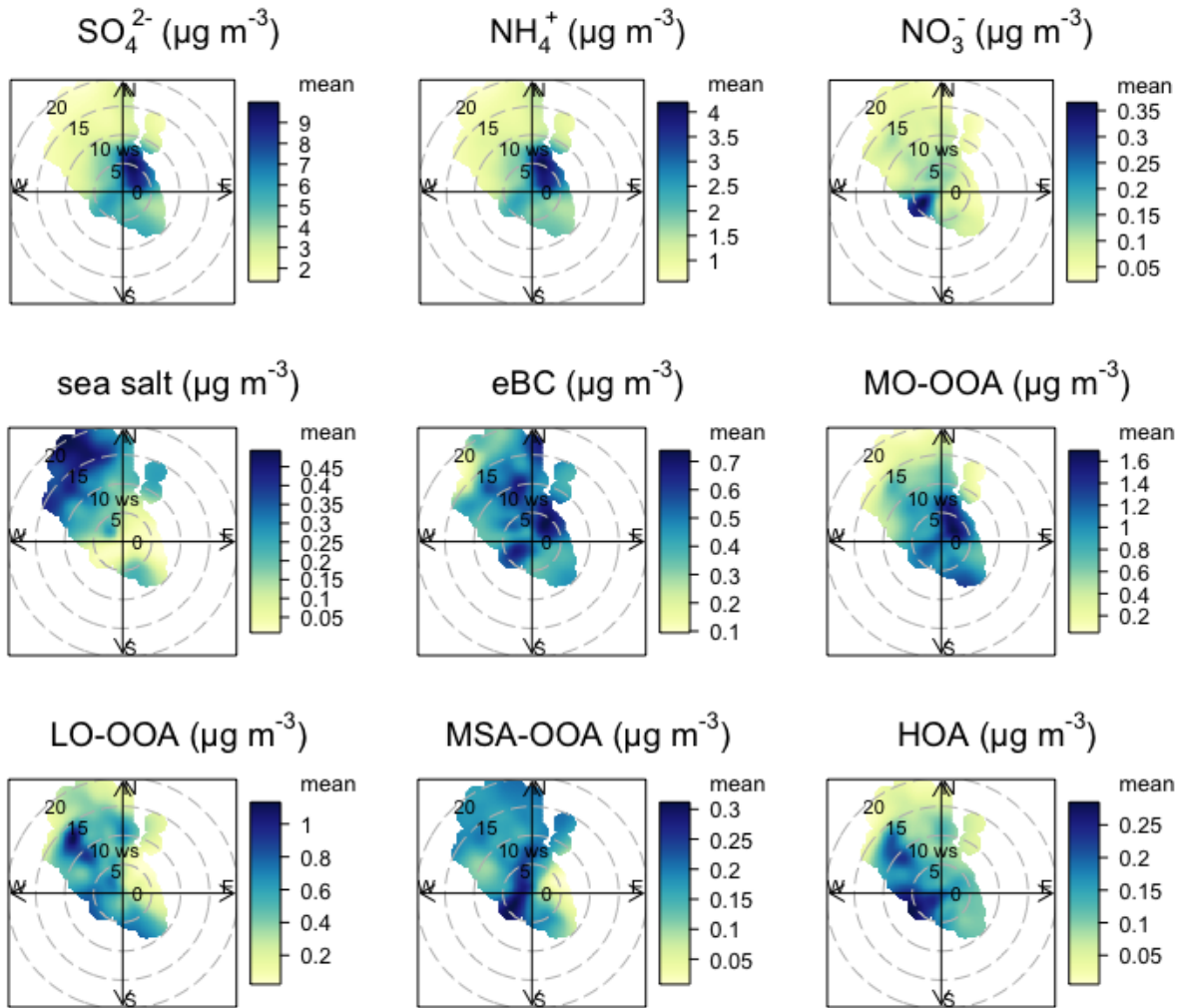
AUTHORS- (YEAR)	LOCATION	PERIOD	INSTRUMENT	PM ₁ MASS AND COMPOSITION	PMF FACTORS
THIS STUDY	Lampedusa (35°31'5"N, 12°37'51"E, 45- m a.s.l.)	10 June - 5 July 2013 (summer)	eToF-AMS	10.1 µg m ⁻³ (OA: 30%, SO ₄ ²⁻ : 44%, NH ₄ ⁺ : 18%, NO ₃ ⁻ : 1%, seasalt: 1%, eBC: 5%)	HOA (8%) MSA-OOA (12%) LO-OOA (28%) MO-OOA (53%)
(MINGUILLÓN- ET AL., 2015)	Montseny (41°46'46"N, 02°21'19"E, 720 m a.s.l.)	June 2012 - July 2013	ACSM	Summer: 10.8 µg m ⁻³ (OA: 60%, SO ₄ ²⁻ : 20%, NH ₄ ⁺ : 0%, NO ₃ ⁻ : 0%, Winter: 6.3 µg m ⁻³ (OA: 8%, SO ₄ ²⁻ : 8%, NH ₄ ⁺ : 0%, NO ₃ ⁻ : 0%)	Summer: HOA (13%) SV-OOA (41%) LV-OOA (44%) Winter: HOA (12%)

					BBOA (28%) OOA (59%)
(ARNDT ET AL., 2017)	Cape Corse (42°58'8.4"N, 9°22'48"E, 544 m a.s.l.)	11 June–6 August 2013 (Summer)	Q-ACSM	5.5 µg m ⁻³ (OA: 55%, SO ₄ ²⁻ : 26%, NH ₄ ⁺ : 13%, NO ₃ ⁻ : 5%)	SV-OOA (62%) LV-OOA (33%)
(MICHOU D ET AL., 2017)	Cape Corse (42°58'8.4"N, 9°22'48"E, 544 m a.s.l.)	July 15–August 5 2013 (Summer)	Q-ACSM	6.8 µg m ⁻³ (OA: 55%, SO ₄ ²⁻ : 27%, NH ₄ ⁺ : 13%, NO ₃ ⁻ : 5%)	HOA (4%) SV-OOA (44%) LV-OOA (53%)
(RINALDI ET AL., 2017)	Cape Granitola (37°34'31.1"N, 12°39'34.2"E, 5 m a.s.l.)	April 2016 (Spring)	HR-ToF-AMS	3.5 µg m ⁻³ (OA: 37%, SO ₄ ²⁻ : 31%, NH ₄ ⁺ : 12%, NO ₃ ⁻ : 3%, seasalt: 10%, BC: 6%)	HOA (3%) BBOA (2%) OOA-1 + OOA-2 (70%) OOA-3 (25%)
HILDEBREANDT ET AL., 2010	Finokalia (35°20'N, 25°40'E, 150 m a.s.l.)	May 2008 (Spring)	Q-AMS	9 µg m ⁻³ (OA: 28%, SO ₄ ²⁻ : 55%, NH ₄ ⁺ : 16%, NO ₃ ⁻ : 2%)	OOA-1 (61%) OOA-2 (39%)
HILDEBRAND ET AL., 2011	Finokalia (35°20'N, 25°40'E, 150 m a.s.l.)	25 February–26 March 2009 (late- Winter)	Q-AMS	3.3 µg m ⁻³ (OA: 43%, SO ₄ ²⁻ : 42%, NH ₄ ⁺ : 14%, NO ₃ ⁻ : 2%)	OOA (>56%) OB-OA (15– 35%) Amine-OA (6– 21%)
BOUGIATIOTI ET AL., 2014	Finokalia (35°20'N, 25°40'E, 150 m a.s.l.)	August– September 2012	Q-ACSM	Fire events: OA: 46.5%, SO ₄ ²⁻ : 29.2%, NH ₄ ⁺ : 11.7%, NO ₃ ⁻ : 3.2%, BC: 9.5% Nonfire periods: OA: 34.7%, SO ₄ ²⁻ : 43%, NH ₄ ⁺ : 13.7%, NO ₃ ⁻ : 2.2%, BC: 6.1%	BBOA (<20%) OOA1-BB + OOA2 (>80%)

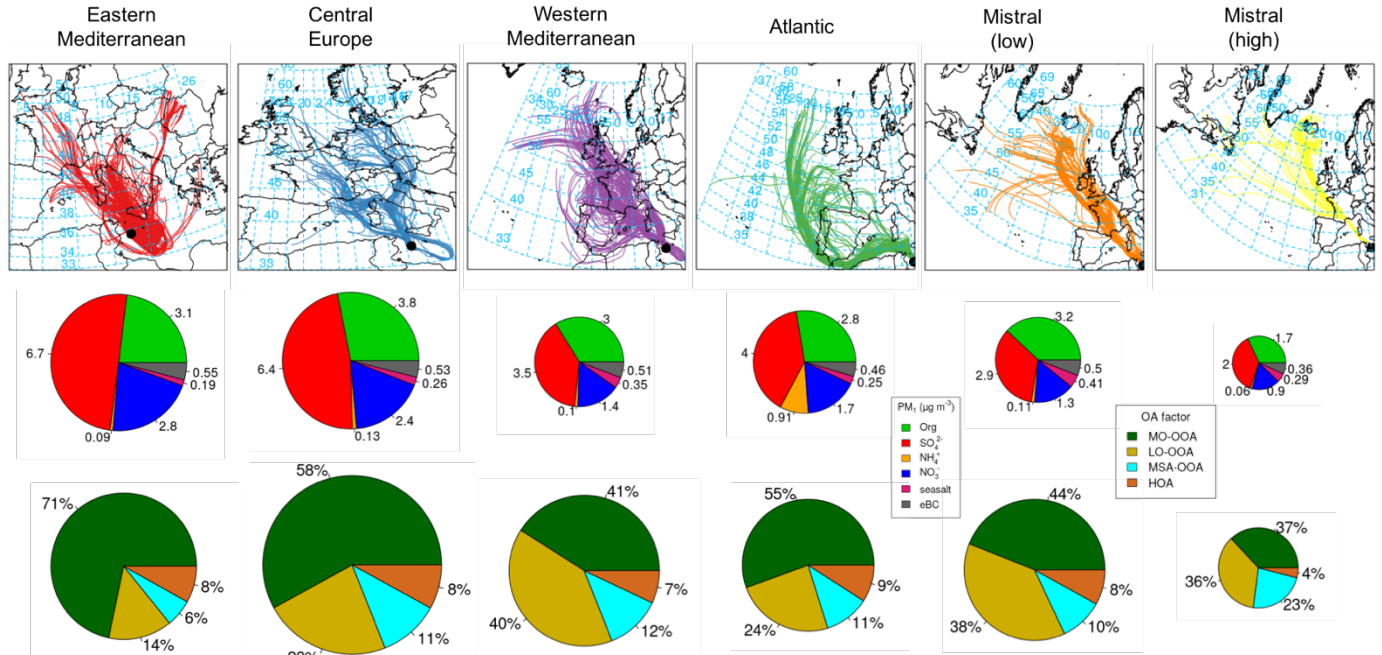


1010

1011 | Figure 98 f_{43} (the ratio of m/z 43 to the total OA) against f_{44} (ratio of m/z 44 to the total OA). The triangle is considered
 1012 to encapsulate typical atmospheric values of OA according to Ng et al. (2010). The values for the various PMF factors
 1013 from this study and other studies conducted in the remote Mediterranean are also displayed.

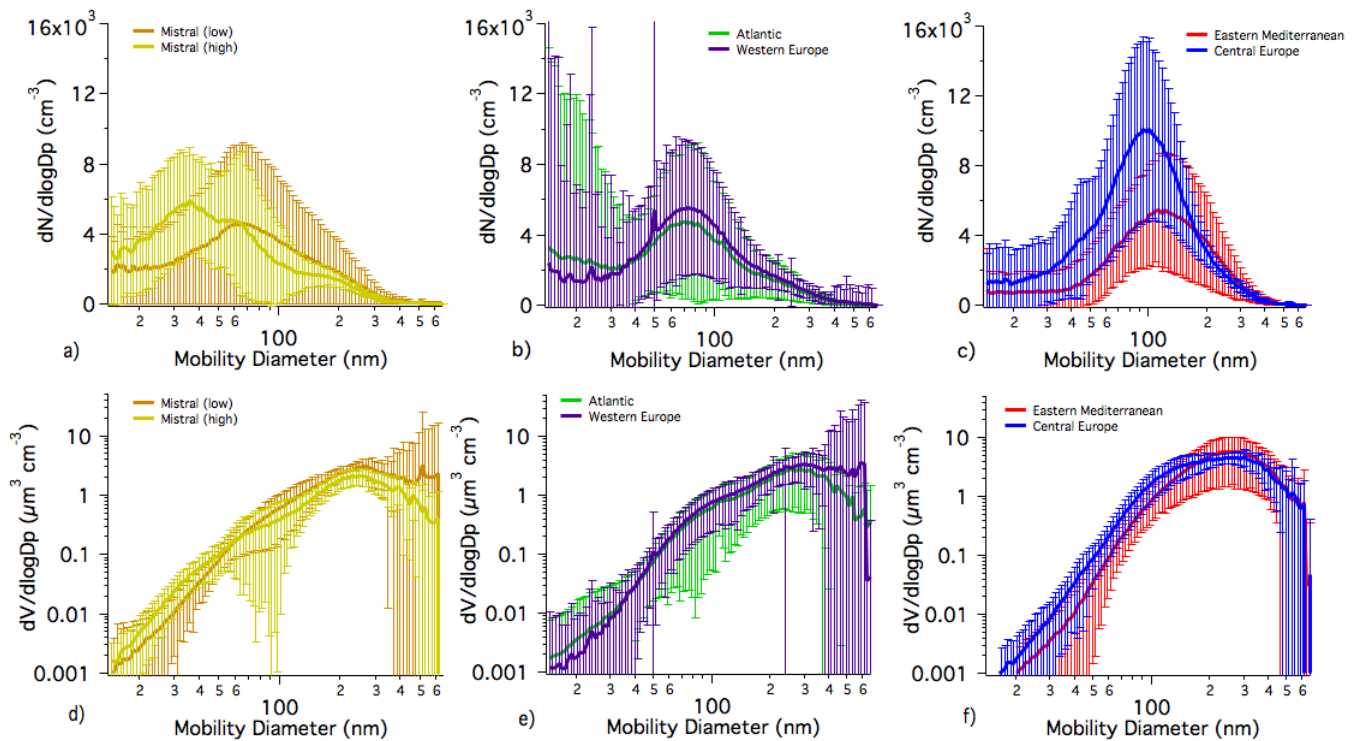


1014
 1015 | Figure 109 Bi-variate polar plots of mean concentrations of PM_1 species and f_{44} at Lampedusa. The angle represents
 1016 the arrival wind direction, the radius represents the wind speed and the colours represent the mean concentrations
 1017 for the respective wind directions and winds.



1018
1019
1020
1021
1022

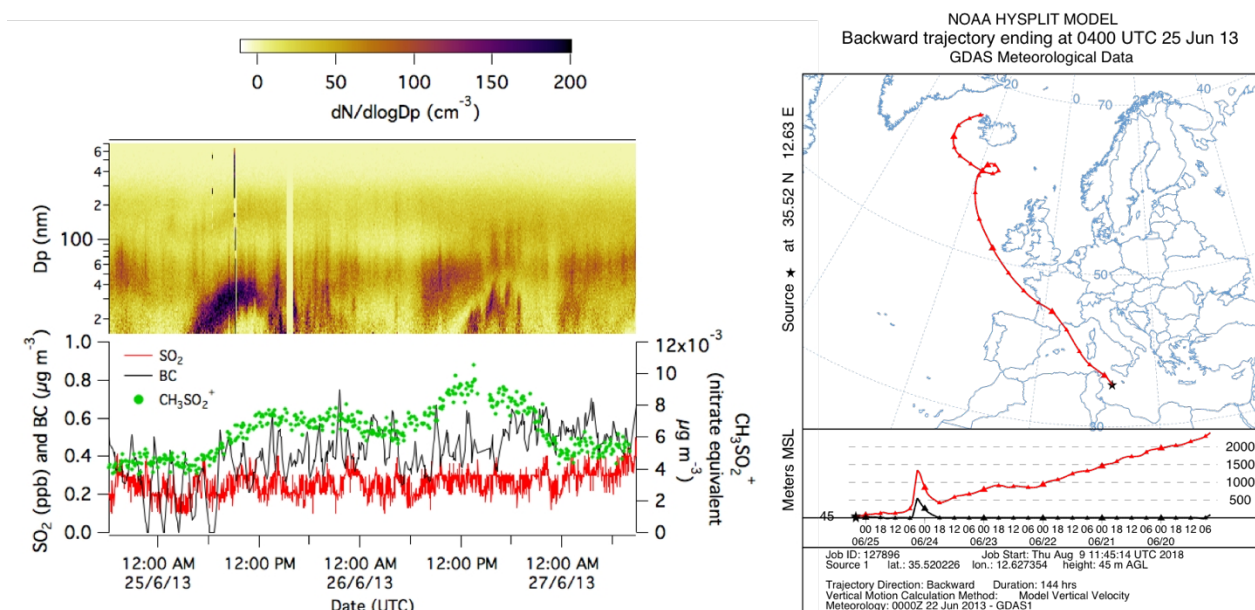
Figure 110 top) 144 hour air mass back trajectories, assigned to each cluster; middle) the PM_{10} composition for each air mass cluster and bottom) the contribution of OA factors for each air mass cluster. The diameter for the PM_{10} composition pie graphs are proportional to the total PM_{10} concentration for each air mass cluster period and the radius for the OA factor pie graphs is proportional to the total PM_{10} organic concentration for each air mass cluster period.



1023
1024
1025

Figure 112 The number size distribution of PM_{10} aerosol, coloured by averages for different air mass origin: a) Mistral (high) and Mistral (low); b) Atlantic and Western Europe; c) Eastern Mediterranean and Central Europe and the

1026 volume size distribution of PM_{10} aerosol, coloured by averages for different air mass origin: d) Mistral (high) and
 1027 Mistral (low); e) Atlantic and Western Europe; f) Eastern Mediterranean and Central Europe.

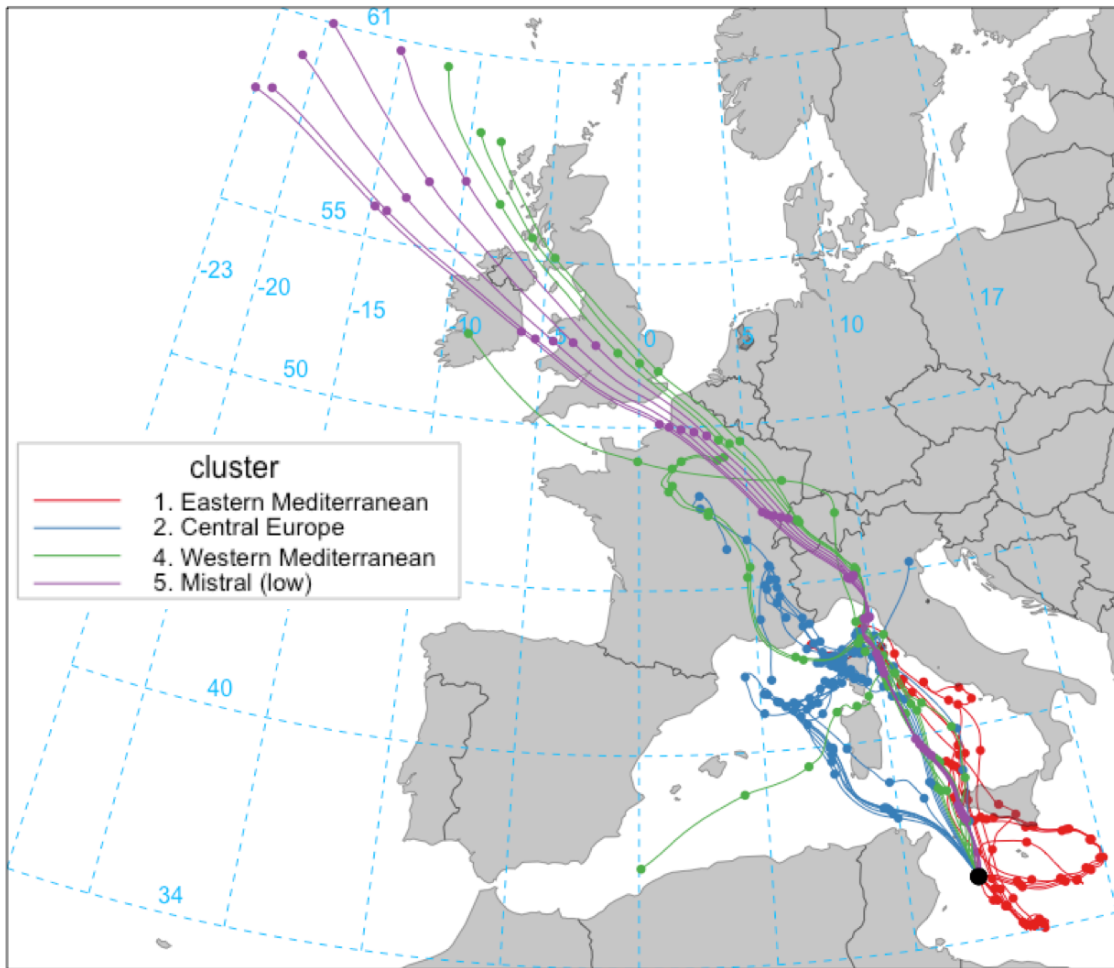


1028
 1029 | Figure 132 (left) The number size distribution during a new particle formation event on 25 June 2013 and the
 1030 corresponding concentrations of SO_2 , eBC and MSA fragment, $CH_3SO_2^+$, and (right) the HYSPLIT air mass
 1031 backwards trajectory during the event.

1032 | Table 12 Campaign average PM_{10} concentration for the major aerosol species measured at the Ersa and Lampedusa
 1033 sites during the SOP-1a period and for periods of coincident air mass backwards trajectories between Ersa and
 1034 Lampedusa

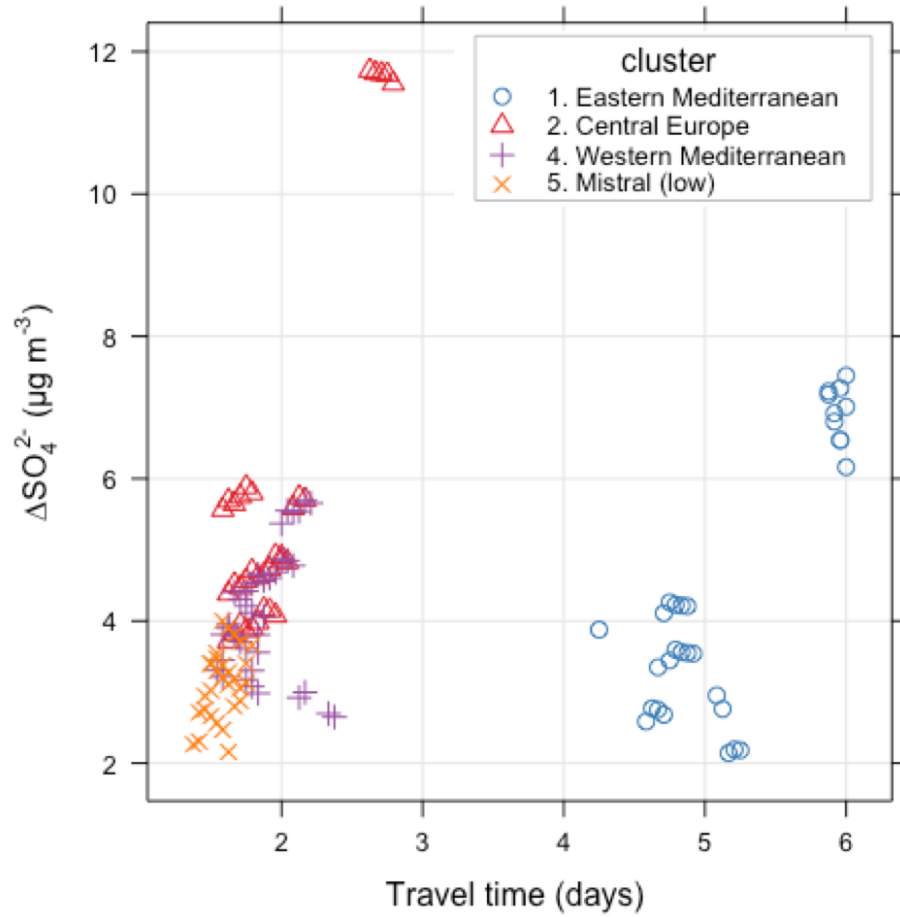
SITE	SO_4^{2-}	ORGANIC	NH_4^+	NO_3^-
ERSA	1.4 ± 2.6	3.0 ± 1.1	0.7 ± 1	0.3 ± 0.1
LAMPEDUSA	4.5 ± 0.9	3.0 ± 1.6	1.9 ± 0.5	0.1 ± 0.2
ERSA (COINCIDENT WITH LAMPEDUSA)	0.9 ± 0.5	2.7 ± 1.1	0.5 ± 0.3	0.4 ± 0.3
LAMPEDUSA (COINCIDENT WITH ERSA)	5.3 ± 2.0	3.8 ± 0.8	2.0 ± 0.6	0.1 ± 0.1

1035



1036
 1037 | *Figure 143 Hourly 120-hour (5 days) backwards trajectories from Lampedusa that passed within $\pm 1^\circ$ in latitude and*
 1038 *longitude and ± 200 m in altitude of the Ersa station. The colours represent the assigned cluster (performed on 144*
 1039 *hour trajectories).*

1040



1041

1042 | *Figure 15 The difference in the $PM_{10} SO_4^{2-}$ mass concentration at Lampedusa and Ersa as a function of the travel time*
 1043 | *of the air masses from Ersa to Lampedusa. Colours represent the air mass origin cluster.*

1044 |